UWB Microstrip Patch Antenna with Reduced Radar Cross Section (RCS)

by

NS Khadija Azmat

Supervisor

Farooq Ahmad Bhatti, PhD

A thesis submitted to the faculty of Electrical Engineering Department, Military College of Signals, National University of Sciences and Technology, Islamabad, Pakistan, in partial fulfillment of the requirements for the degree of MS in

Electrical Engineering

AUGUST 2020

THESIS ACCEPTANCE CERTIFICATE

Certified that final copy of MS thesis written by Ms. **NS Khadija Azmat**, Registration No.**00000117634** of Military College of Signals has been vetted by undersigned, found complete in all respect as per NUST Statues/Regulations, is free of plagiarism, errors and mistakes and is accepted as partial fulfillment for award of MS degree. It is further certified that necessary amendments as pointed out by GEC members of the student have been also incorporated in the said thesis.

Signature: _____

Name of Supervisor: **Farooq Ahmad Bhatti, PhD**

Date: _____

Signature (HoD):_____

Date: _____

Signature (Dean):_____

Date: _____

ABSTRACT

The UWB platform has undergone several advances over the past decades due to its promising applications in both the military and commercial spheres. Due to its very-low profile, light weight, low transmission power, simplicity of fabrication and low manufacturing cost, the UWB Micro-strip antennas have extensive applications. With the massive growth in radar and stealth technology, Radar Cross Section (RCS) reduction is becoming ever more essential area of research. Antenna plays a significant role in adding up the overall RCS to the system as compared to the other communication devices. Nonetheless, RCS reduction is a challenging task to attain for the wide frequency range due to the degradation of performance of antenna in terms of its gain and radiation pattern. A enormous number of applications require not only good radiation pattern antenna but also reduced RCS.

In this research, an antenna with frequency selective surface (FSS) is proposed which covers Ku/K frequency band 12-20 GHz. The simulated results has been compared with the measured results and good consent has been observed. The measure peak gain at 17.5 GHz is 8.1 dB. The maximum monostatic RCS -87.5 dBsm has been observed at 15.2 GHz wheras, minimum RCS -67.6 dBsm has been observed at 20 GHz. The proposed antenna with FSS is compact as compared with the existed literature.

DEDICATION

Dedicated to
Abu and Ammi, for their love and support throughout my life and to my sisters Tayyaba Azmat and Fatima Azmat who always believe in me and helped me to be a better version of myself, and to my respected teachers without them none of this could ever be possible and to my MS colleagues for their continue support and motivation.

ACKNOWLEDGEMENTS

I am thankful to Allah Almighty (all praise belongs to Him) for giving me the strength and ability to achieve my objectives and successfully complete this research work.

I am highly grateful to my supervisor, Dr. Farooq Ahmad Bhatti for guiding and supporting me throughout my research work. His timely encouragement has led me to complete this research successfully. He not only imparted significant knowledge to me but also contributed extensively in my work. I am highly obliged to my Guidance and Evaluation Committee (GEC) members as well, that included Dr. Zeeshan Zahid and Ma'am Maryam Rasool for dedicating their precious time for my research work and always guiding me through it.

Finally I would like to pay my gratitude to all those people without whom I could never have accomplished my aim including my family, especially my parents and my teachers. I am grateful to them for their constant prayers and persistent support throughout this journey. May Allah bless them all with eternal happiness.

TABLE OF CONTENT

THESIS ACCAEPTANCE CERTIFICATE ..... **i**
ABSTRACT ..... **ii**
DEDICATION ..... **iii**
ACKNOWLEDGEMENTS ..... **iv**
LIST OF FIGURES ..... **vii**
LIST OF TABLES ..... **x**
ACRONYMS ..... **xi**
INTRODUCTION **1**
1.1. Background 1
1.2. Research Motivation 4
1.2.1. Problem Statement 4
1.2.2. Aims and Objectives 4
1.3. Applications 4
1.4. Advantages 5
LITERATURE REVIEW **6**
2.1. UWB ANTENNAS 6
2.1.1. Rectangular Shape 6
2.1.2. Rectangular shape antenna with Rounded Edges 8
2.1.3. Circular Shape antenna 9
2.1.4. Rectangular and Circular combine Shape antenna 11
2.1.5. Elliptical Shape antenna 12
2.1.6. Triangular Shape antenna 13
2.1.7. Hexagonal Shape antenna 15
2.1.8. Octagonal Shape antenna 16
2.1.9. Diamond Shape antenna 17
2.1.10. Random Shape antenna 18
2.2. Frequency Selective Surface 19
2.2.1. Hexagonal elements 20
2.2.2. Combination elements 20
2.3. Radar Cross Section (RCS) Reduction 23
2.3.1. Planar Octagonal-Shaped UWB Antenna 24
2.3.2. Low RCS Micro-strip Patch Antenna Using Frequency-Selective Surface and Micro-strip Resonator 25

2.3.3. Wideband radar cross-section reduction of micro-strip patch antenna with split-ring resonators 26
2.3.4. Ultra Wideband Antenna with Reduced Radar Cross Section 27
2.3.5. Radar Cross Section Reduction of a Micro-strip Antenna Based on Polarization Conversion Meta-material 28
2.3.6. Gain Enhancement and RCS Reduction for Patch Antenna by Using Polarization Dependent EBG Surface 29
2.3.7. Radar Cross Section Reduction of Micro-strip Antenna Using Dual-Band Meta-material Absorber 30
2.3.8. In-Band RCS Reduction and Gain Enhancement of a Dual-Band PRMS-Antenna 32
2.3.9. Broadband RCS Reduction of Micro-strip Antenna Using Coding Frequency Selective Surface 33
SIMULATION OF UWB ANTENNA WITH FSS 35
3.1 UWB Antenna 35
3.2 Antenna for Ku/K band Applications 36
3.2.1 Parametric Study 37
3.2.2 Analytical Design 38
3.2.3 Design of FSS 41
3.2.4 Antenna with FSS 45
DESIGN ANALYSIS OF ANTENNA WITH FSS 53
4.1 Antenna Design 53
4.2 FSS Design 55
4.3 Antenna with FSS 56
CONCLUSION AND FUTURE WORK 59
5.1 Discussion 59
5.2 Conclusion 59
5.3 Future work ..... **Error! Bookmark not defined.**
BIBLIOGRAPHY ..... Error! Bookmark not defined.

LIST OF FIGURES

Figure 2.1: UWB Micro-strip patch Antenna with Rectangular shape…… 07

Figure 2.2: Radiation Pattern…….. 07

Figure 2.3: UWB Micro-strip Antenna with rounded edges…… 08

Figure 2.4: Radiation Pattern…… 09

Figure 2.5:UWB Antenna with circular shape……. 10

Figure 2.6: UWB Antenna with both circular and rectangle shape..……... 11

Figure 2.7: Gain versus Frequency……..…..... 12

Figure 2.8:UWB Antenna with elliptical shape……..... 12

Figure 2.9: Gain and Efficiency versus Frequency…… 13

Figure 2.10:UWB antenna with triangular shape……... 14

Figure 2.11: Radiation pattern at frequency of 4.27 GHz…….... 14

Figure 2.12: Hexagonal Shape for UWB Antenna…… 15

Figure 2.13: Gain versus Frequency plot……... 15

Figure 2.14: Octagonal Shaped UWB antenna…… 16

Figure 2.15: Radiation patterns of octagonal UWB antenna……..... 17

Figure 2.16: Diamond Shaped UWB antenna…… 18

Figure 2.17: Radiation pattern at 17.5 GHz…….....…. 18

Figure 2.18: Random Shaped UWB Antenna…… 19

Figure 2.19: Geometries of patch and aperture type elements FSS array [26].……. 19

Figure 2.20: Unit cells of FSS element geometries [27].……..... 20

Figure 2.21: (a) Patch type and (b) slot type periodic structures with their surface impedance, 22

the response of the patch array is capacitive and that of slot type is inductive [29]……..

Figure 2.22: (a) Short dipole type FSS surface (b) Long strips type FSS surface…… 23

Figure 2.23: Octagonal-shaped UWB antennas. (a) Reference. (b) Modified……. 25

Figure 2.24: (a) Top and (b) bottom view of two fabricated antennas……. 26

Figure 2.25: Reference and proposed antennas a)Top view b) Bottom view…….. 27

Figure 2.26: Fabricated prototypes Top view (left) and bottom view (right)……. 28

Figure 2.27: Simulation results of mono-static RCS for x-polarized incident wave impinging…… 28

Figure 2.28: Reference and proposed antennas: (a) top view (b) bottom view……. 29

Figure 2.29: Photograph of fabricated slot-EBG antenna prototype…… 30

Figure 2.30: Simulated and measured RCS reduction versus frequency forx-andy-polarization plane waves…….. 30

Figure 2.31: Micro-strip antenna with dimensions of:Lp = 14.6 mm,Wp = 10.6 mm, Ls = 52.5 mm, Ws = 52.5 mm, l4 = 2.9 mm,and d = 0.8 mm…….. 31

Figure 2.32: Configuration of low RCS micro-strip antenna (a) Side view and (b) top view……..... 32

Figure 2.33: Simulated mono-static RCS of micro-strip antenna with and without absorber at under normal incidence at: (a) 8.4 and (b) 11.1 GHz…….. 32

Figure 2.34: Fabrication of the proposed antenna……. 33

Figure 2.35: Measurement results of RCS reduction for both polarizations under normal 33

Figure 2.36: Low RCS Antenna using one bit coding FSS in ground plane. (a) Top view. (b) Bottom view……... 34

Figure 2.37: Comparison of mono-static RCS between measured and simulated of the reference and proposed antennas in the frequency range of 6 GHz-12 GHz……. 34

Figure 3.1 UWB Antenna (a) front view (b) back view…….. 38

Figure 3.2 Reflection of UWB antenna……. 39

Figure 3.3 3D Gain Plot of UWB antenna at 5.7 GHz…….. 39

Figure 3.4 VSWR of UWB antenna……. 40

Figure 3.5 Design of unit cell with parameters (a=b=2.25mm, c=d=1.5mm, e=f=0.75mm, g=h=0.75mm, p=7.5mm)…….. 41

Figure 3.6 Unit cell with Floquet ports assigned…….. 42

Figure 3.7 Reflection coefficient of single unit cell…… 43

Figure 3.8 Frequency selective surface (FSS) 8×8 array…… 44

Figure 3.9 Reflection coefficient of FSS array…… 44

Figure 3.10 8×8 patch antenna with FSS array…….. 45

Figure 3.11 S-Parameters of antenna with FSS…….. 45

Figure 3.12 3D Gain plot of antenna with FSS at different heights 19GHz…… 46

Figure 3.13 RCS plot for theta 90° (a) 16 GHz and (b) 20 GHz…….. 47

Figure 4.1 Fabricated UWB Antenna (a) Front View (b) Back View……. 48

Figure 4.2 UWB Antenna simulated and measured results……. 49

Figure 4.3 Peak gain of UWB Antenna without FSS…….. 49

Figure 4.4 Fabricated 8 × 8 frequency selective surface (FSS)…….. 50

Figure 4.5 Antenna with FSS at a seperation distance of 4 mm……. 51

Figure 4.6 Peak gain of antenna with FSS…….. 51

Figure 4.7 Monostaic radar cross section of antenna with FSS……. 52

Figure 4.8 3D RCS of antenna with FSS at 16 GHz……. 52

LIST OF TABLES

Table 2.1: Circular Shape antenna parameters with results……. 10

Table 4.1 Comparison of proposed work with the existed literature…… 58

ACRONYMS

Ultra Wideband	UWB
Radar Cross Section	RCS
Radar Absorbing Material	RAM
Electro-magnetic Gap	EBG
Artificial Magnetic Conductor	AMC

CHAPTER 1

INTRODUCTION

1.1 Background

Ultra Wide Band (UWB) forms the basis of almost all the different methods used by the wireless communication systems. Heinrich Hertz invented the first spark gap transmitter in 1886 after having tested the Maxwell's Equations. In 1896, first ever communication system of UWB was created in London. The aim of this system was to connect two post offices that were far from each other [1]. A UWB program was also introduced in 1960 which essentially enabled the U.S. armed forces to use pulses to ensure radar and stealth communication [2]. In 2002, Ultra Wide Band (UWB) technology was released by the Federal Communication Commission (FCC) for commercial applications [3]. The most significant feature of UWB framework is that it may classify its channel capability as bandwidth. As the bandwidth of a UWB system is ultra-wide, it is capable of handling massive quantities of data rate. UWB will be able to traverse many license carrier-based transmissions after having the capability to handle substantial amounts of bandwidth. One of the biggest assumptions presumed by everyone about UWB transmissions is that it may result in interference. UWB systems have the potential to operate at extremely low power levels and therefore have low spectral density. This characteristic is attributed largely to the wide bandwidth. It can provide reliable and good communication system, as the chances of sudden detections are reduced due to low energy density. The regulatory authorities specifically restricted the power limits for UWB. They are so low on few occasions that they are even lower than the spurious electronic appliance emissions. Keeping this in mind, it is presumed that UWB

transmission will not cause any noticeable interference to other licensed users. Besides this, the regulatory authorities are ensuring that other user's transmission and performance is not being affected [4]. Owing to the promising applications of UWB antennas in the areas of wireless communication including high data rate, microwave imaging systems and high accuracy radar, a significant amount of research has been done on them over the past few decades. The need to spread UWB technology in comparison with other narrow band technologies requires the relatively small size and broad impedance bandwidth antennas. The micro-strip patch antennas are the most widely used antennas for the UWB systems because of their wide range of applications. Patch antennas typically have simple structure, very low profile, light weight, ease of fabrication and low cost of production compared to other antennas [5]. With the rapid growth of the stealth technologies and the development of the radar systems, the Radar Cross Section (RCS) of devices has gained much attention. Due to the advancement of stealth technology, the Radar Cross Section (RCS) has gained increasing attention over the past few years, particularly for military applications. In communication platform, a significant role is played by the antenna on one hand but on the other hand, it is a major contributor in adding up the overall RCS. Over the past few years, numerous techniques have been proposed for the reduction of the RCS of antenna in different frequency bands, but these techniques have degraded the gain of antenna and its radiation efficiency. The challenge is to reduce the antenna RCS without degrading its performance, and make it efficient for stealth and other military applications. Hence, it is a challenging task to reduce the RCS of antenna without degradation of its performance and at the same time, making it efficient for the stealth and various other military applications.

Various methods have been proposed for the reduction of RCS of the system. One of them is by reducing the number of antennas being utilized in the system. Since the RCS is

directly linked to the antennas, therefore the overall RCS will be reduced by cutting off the number of antennas [6].

The most widely used approaches to reduce the RCS of antenna are by changing the shape of the antenna, by coating the Radar Absorbing Material (RAMs) on the antenna surface or cancellation using active and passive technology [7]. However, these approaches degrade the overall performance of the antenna [7]. The primary aim of using the absorbent material is to absorb the Electro-magnetic (EM) waves and convert them into heat [8]. The purpose of modifying the shape of the antenna is to make it capable of reflecting the energy of EM waves in a direction other than the incidence direction [8]. Passive cancellation technique has also been proposed in some of the research papers for the reduction of RCS of antenna by means of the hybrid AMC structures with the combination of micro-strip patch antenna [9]. This technique is however mainly effective for micro-strip patch antennas and slotted antennas only [8]. Another method of reducing the RCS of antenna is by using the meta-material surface, these meta-material surfaces are polarization-dependent, EBG elements in the slotted form are used to improve the overall gain of the antenna [9]. However, this approach has some drawbacks, it improves the overall antenna gain, but it is only effective for the large ground plane when the ground plane are low in size, the antenna efficiency reduces significantly [10]. In [11], absorbing material is used with the combination of partially reflecting surface in order to reduce the RCS of antenna and enhancing its gain. The antenna achieved both the in band and out of band RCS reduction. Another method for RCS reduction is by the use of Hybrid Absorber material that is wideband electro-magnetic, the design is based on the meta-material covered by the hybrid absorber material [12]. This approach, however, has a drawback in terms of radiation performance and an antenna gain [13].

1.2 Research Motivation

1.2.1 Problem Statement

Due to the advancement of stealth technology, particularly for military applications, the Radar Cross Section (RCS) has gained more and more attention over the past few years. Antenna plays a very significant role in platform communication but antenna also makes an immense contribution to adding up the overall RCS. Over the past few years, numerous techniques have been proposed for RCS reduction in different frequency bands, but these techniques have degraded the performance of antenna in terms of its gain and radiation performance. Hence, it is a challenging task to reduce the RCS of antenna without degrading its performance and making it efficient for the stealth and other military applications.

1.2.2 Aims and Objectives

The aim of this research is to design a micro-strip patch antenna with the following goals:

- To cover the Ultra Wide Band (UWB).
- To reduce Radar Cross Section (RCS) of the antenna without effecting its overall performance.

1.3 Applications

UWB technology can be used in enormous applications that can be categorized among data and voice to radar and tagging. Although there has been plenty of hype about using UWB ultra wideband in commercial applications, these systems are equally important in military applications. Among several other benefits, a significantly important one is that the pulses being spread over a wider range of spectrum will be difficult to detect which makes this idea suitable for use in covert communications.

The proposed antenna will be efficient for stealth applications making it invisible to radar and other detecting devices. Furthermore, it will be useful for military platforms as well while saving the overall budget.

The commercial applications are illustrated below.

- Higher speed LAN / WAN (>20 Mbps)
- Radar Avoidance
- Altimeter (aviation)
- Intelligent transport systems tags
- Detection of any Intrusion
- Geo-localization

The military applications include:

- Radar
- Furtive communications
- Intrusion detection
- Precision geo-location
- Data links

1.4. Advantages:

This research will prove to be certainly useful in many perspectives, such as:

- Designing of Low Observable antenna
- Gain enhancement
- Maintaining the overall performance of the antenna

CHAPTER 2

LITERATURE REVIEW

2.1 UWB ANTENNAS

UWB technology has been extensively used in many applications owing to its high data transmission rate, improved bandwidth and short-range characteristics. Applications such as Wireless Personal Area Network (WPAN), Wireless Body Area Network (WBAN), indoor, geo-localization and biomedical imaging exploit the UWB technology. Designing UWB antennas for these applications is still a challenging task which has attracted many researchers. UWB antennas are designed in different shapes e.g. rectangular, triangular, circular, elliptical, hexagonal, octagonal, diamond and some random shapes, in order to meet the requirements of the different applications.

2.1.1 Rectangular Shape

In order to meet the requirements of UWB applications, a rectangular shaped antenna is presented with compact size and good impedance characteristics. Parameters of the antennas can be varied to improve the impedance bandwidth. The ground plane is cut in the form of slots, as shown in Figure 2.1, in order to obtain a symmetrical saw tooth shape. This design was implemented with a rectangular shape from the top and a modified ground having a saw tooth shape. In figure 2.1a , the implemented design is shown while its prototype is shown in Figure 2.1b.

The results obtained by this design are shown in Figure 2.2. It can be seen that the measured radiation patterns of the two planes i.e xz-plane and yz-plane respectively, is at 3.6,

7.2 and 9.6 GHz. The first pattern illustrates the xz-plane whereas the second one is for the yz-plane. From the radiation patterns it can be observed that yz-plane patterns are omni-dimensional patterns whereas xz-plane patterns are monopole like patterns. Micro strip feed line is printed directly onto the slotted partial ground plane which could be the reason behind few dips observed in the radiation pattern. Nevertheless, for the operating band, the radiation pattern is stable everywhere [14].

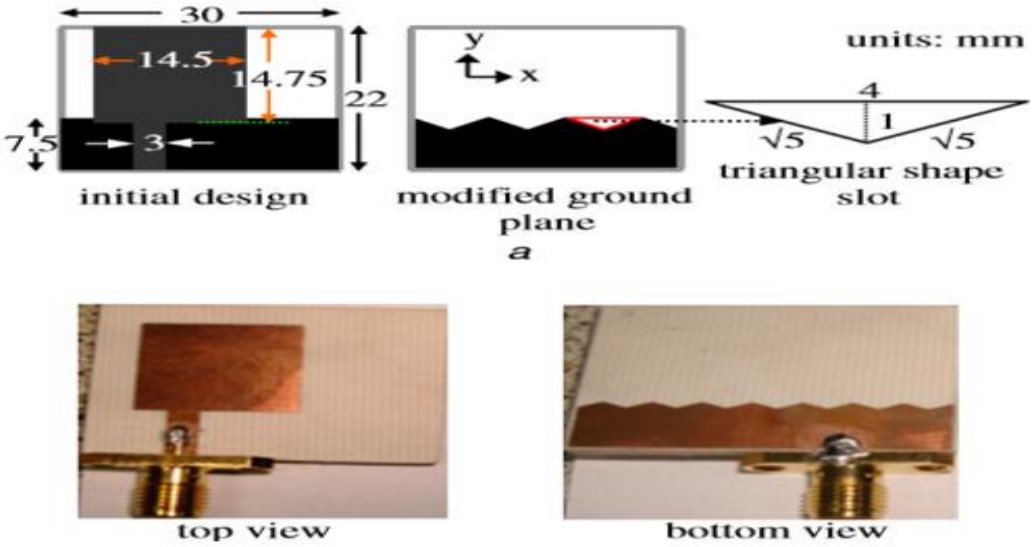

Figure 2.1: UWB Micro-strip patch Antenna with Rectangular shape

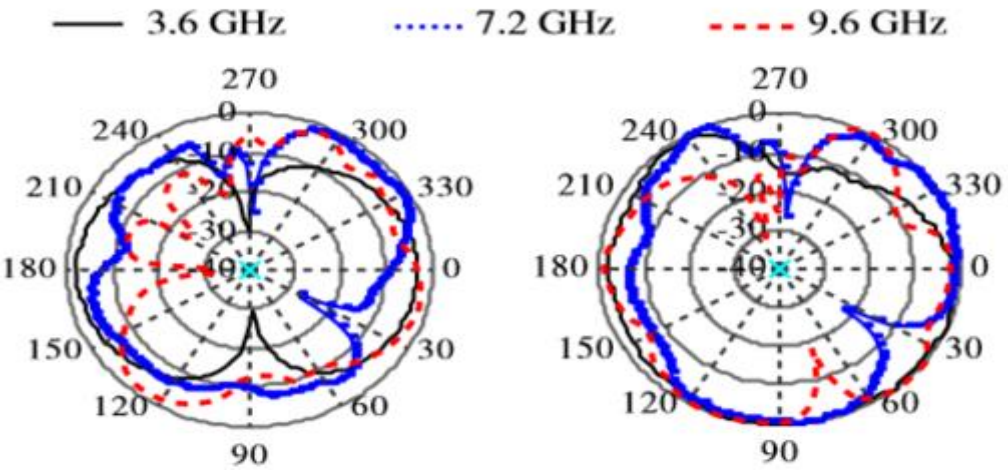

Figure 2.2: Radiation Pattern

2.1.2 Rectangular shape antenna with Rounded Edges

In order to achieve the requirements of various UWB applications and cognitive radio, this simple and low profile antenna was proposed. Numerous modifications were made in the conventional rectangular shaped antenna in order to obtain this design. The foremost advantage of these modifications is achievement of an increased bandwidth. The ground plane of the traditional antenna was essentially truncated to cause a reduction in Q factor [15]. Due to the truncated ground, the impedance between the micro strip antenna and its feed line can also be increased which enhances the bandwidth further. The purpose of round junction was to bring about a smooth variation in the impedance between the transmission line and the antenna patch. This smooth variation allows the reflection coefficient to be reduced thus increasing the bandwidth. The final step is to chamfer the last two corners of the radiating antenna element.

In figure 2.3, another type of UWB antenna having a truncated ground plane, round junctions and two chamfers, is illustrated. The chamfers serves the purpose of providing impedance matching at 27 and 29 GHz.

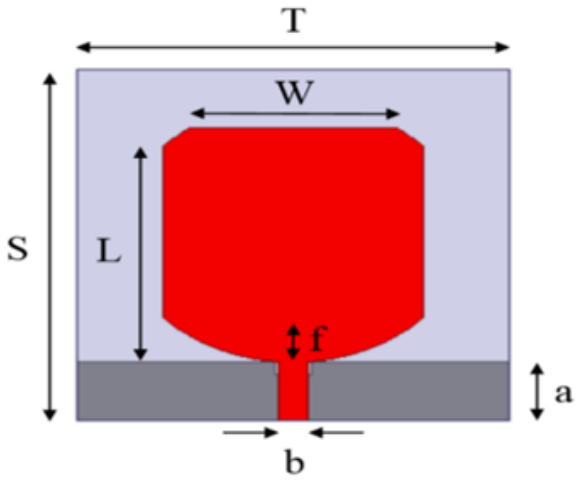

Figure 2.3: UWB Micro-strip Antenna with rounded edges

The radiation patterns obtained by the aforementioned UWB antenna is depicted in Figure 4. The radiation pattern obtained at 2 GHz is shown by blue continuous lines, the dashed red lines show the radiation pattern obtained at 14 GHz whereas the black curves with circles depict the radiation pattern at 28 GHz. Furthermore, figure 2.4a demonstrated the parallel plane radiation pattern and figure 2.4b demonstrated the perpendicular plane radiation pattern. At 2 GHz, an omnidirectional pattern is obtained in the azimuth plane and a maximum gain of 2.2 dBi is achieved. For 14 GHZ and 28 GHz frequency bands, random distributed patterns are obtained. This randomness can be attributed to the increasing modes of propagation. The maximum gain obtained from dashed red lines and black curves are 6.8 and 8.53 dBi respectively [16].

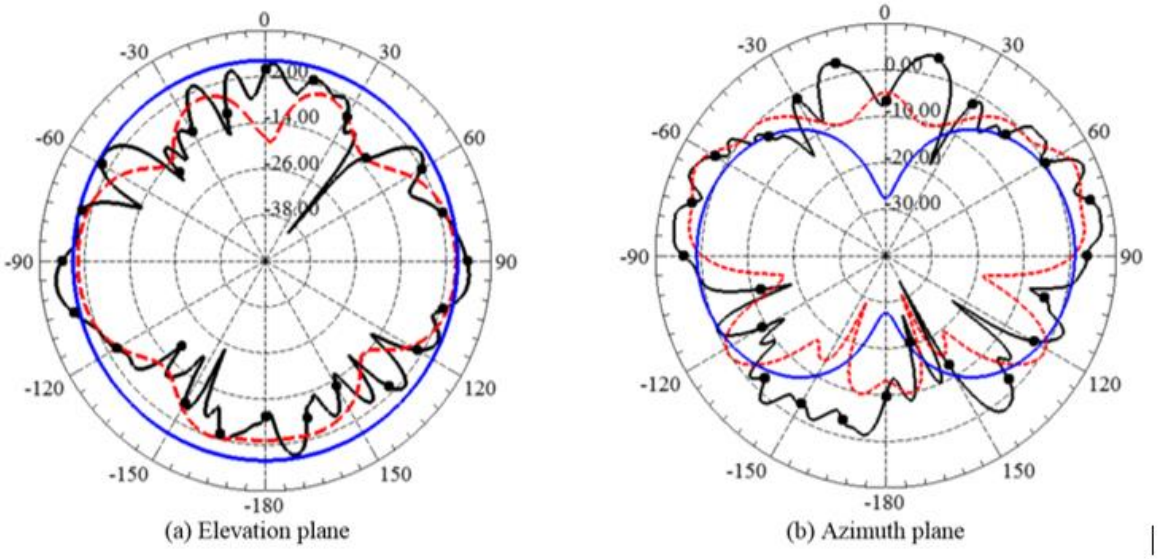

Figure 2.4: Radiation Pattern

2.1.3 Circular Shape antenna

Circular shape antennas are generally used in low profile antennas applications. In literature, there are several shapes for patch antennas but compared to other shapes, the

circular shape patch antenna has far more advantages over them. Among these advantages are the design flexibility, maximum bandwidth achievement, good radiation pattern, improved directivity and better return loss [17]. This antenna uses FR4 as substrate and is comprised of a conducting patch and a ground plane. Different dimensions are used for the thickness of substrate, ground plane and the feed line.

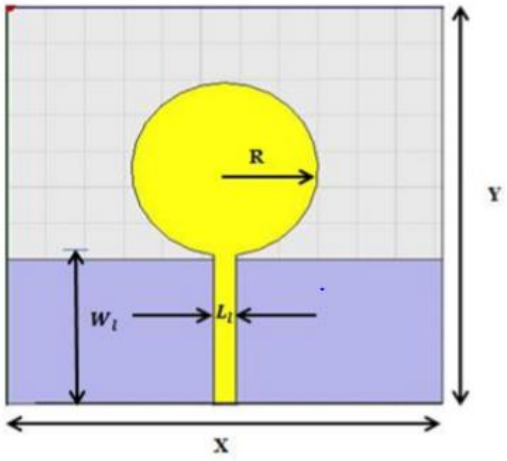

Figure 2.5:UWB Antenna with circular shape

The results of the circular shaped UWB antenna are given in Table 1. It shows that the antenna parameters like VSWR and gain gives satisfactory performance. Furthermore, the addition of partial ground has further enhanced the radiation characteristics. Therefore, this design is suitable for multi-band wireless communication [18].

Antenna Parameters	Circular Shape
Resonant Frequency	6.3 10.22
Return Loss (dB)	-19.3391 -24.0508
Gain (dBi)	4.0503 5.5311
VSWR	1.2554 1.1195

Bandwidth (GHz)	1.6-11.6 (10 GHz)

Table 2.1: Circular Shape antenna parameters with results

2.1.4 Rectangular and Circular combine Shape antenna

The combination of a rectangular and circular shape provides a unique design, resulting in a combined shape. For this purpose, the rectangular and circular monopole antennas are implemented independently. The best impedance matching is obtained when the feed line is 5mm away. Both the shapes were then combined in order to obtain a rectangular and circular shaped UWB antenna as shown in Figure 2.6.

Figure 2.6: UWB Antenna with both circular and rectangle shape

Figure 2.7 shows the gain along with the frequency obtained from simulations as well as measurements. From the graph, it can be concluded that this shape of antenna yields a bandwidth of more than 8 GHz ranging from 1 GHz to 10 GHz. Furthermore, some variation is shown by the gain in the broadside, that is, from 1 dBi to 3 dBi. Such type of randomly shaped antenna can be utilized in applications such as personal mobile communication, Bluetooth, WiFi but only for the range of 1 GHz to 10 GHz [19].

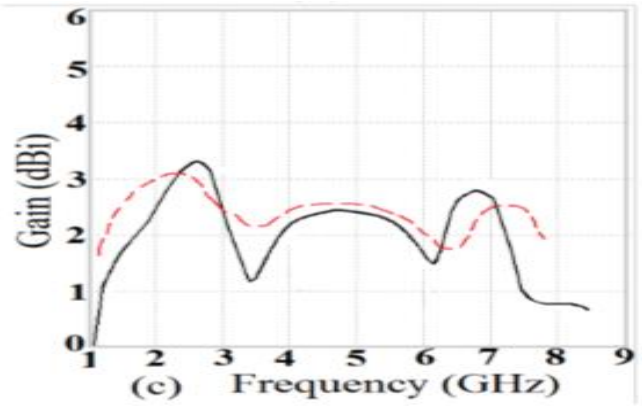

Figure 2.7: Gain versus Frequency

2.1.5 Elliptical Shape antenna

This is basically an elliptical monopole antenna, as shown in Figure 2.8, with the ground plane in a trapezoidal shape and fed by a modified tapered CPW line. Measurement results show that a wide impedance bandwidth can be achieved. Various wireless services such as GPS, GSM 1800,PCS 1900,GNNS and UWB etc. can be supported by this type of elliptical shaped antenna.

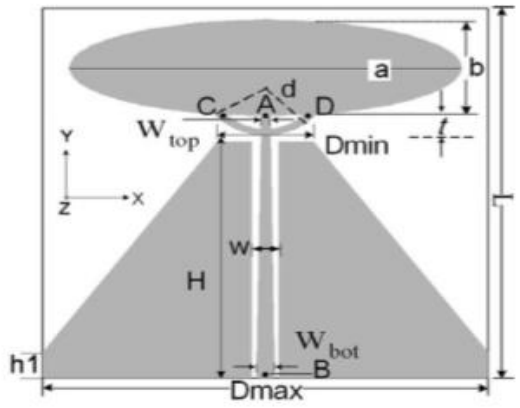

Figure 2.8:UWB Antenna with elliptical shape

For acquiring efficient results, two feeding branches are installed, which optimize the radiating elliptical patch and the ground plane. Furthermore, the elliptical patch and the ground plane are

attached on the same side of the substrate. In Figure 2.9, the graph of the antenna gain and efficiency is shown at frequencies 1, 5, 10, 15 and 20 GHz. It can be observed that there are some fluctuations in the gain. Initially there is a gradual increase in gain until 15 GHz and after 15 GHz, there is a drop in the gain. Furthermore, for the low range of frequencies, the radiation efficiency is approximately constant however it drops eventually giving a value of 76% at 20 H. This drop in the gain and efficiency is because of the loss of frequency in the RF substrate. With the increase in frequency, the antenna begins to operate in higher order modes instead of the base mode which results in severe degradation of the performance of elliptical shaped antenna in the far field region. Therefore, there is a decrease in gain with an increase in frequency [20].

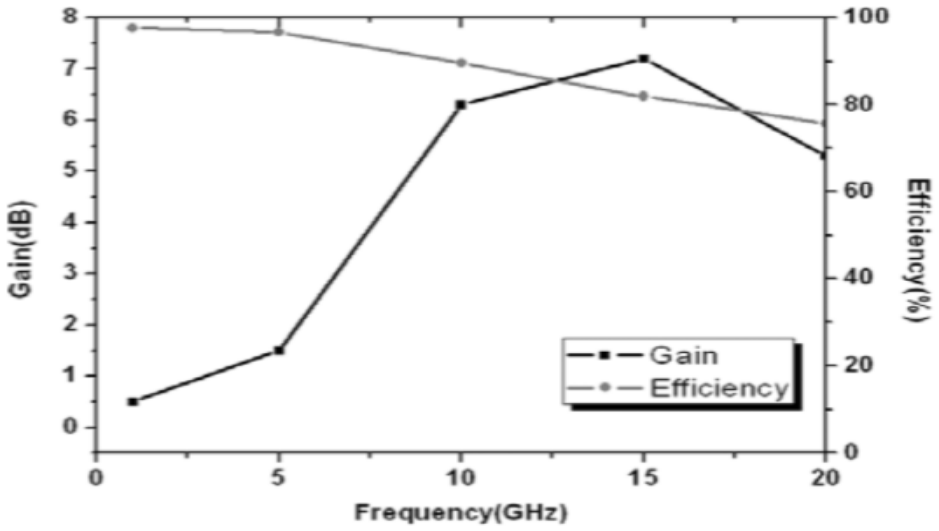

Figure 2.9: Gain and Efficiency versus Frequency

2.1.6 Triangular Shape antenna

This antenna is made up of a triangular monopole antenna with a tapered CPW feed line. By using this type of feed line, the bandwidth of the CPW-fed can be increased. The gap between the ground plane and the feed line is kept 0.1 mm.

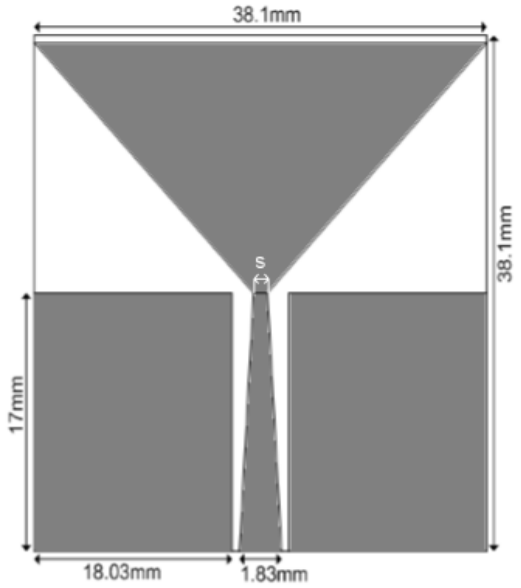

Figure 2.10:UWB antenna with triangular shape

Figure 2.11 shows the radiation pattern in E-plane at a frequency of 4.27 GHz. It can be observed that the radiation pattern is mostly omnidirectional. As the frequency increases, the cross-polarization level rises. Such an antenna design can be used in multi-path environments [21].

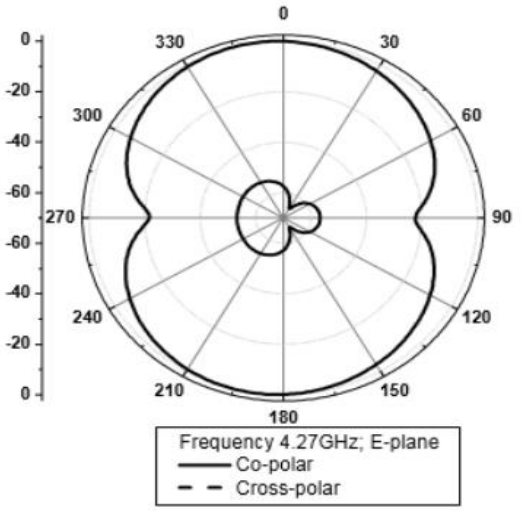

Figure 2.11: Radiation pattern at frequency of 4.27 GHz

2.1.7 Hexagonal Shape antenna

This is a CPW-fed hexagonal shape antenna design having the band notch characteristics of WLAN and WiMAX. Initially, the design is constructed with a simple hexagonal antenna and the band notch characteristics are then added afterwards [22]. The prototype of this hexagonal antenna design is shown in Figure 2.12.

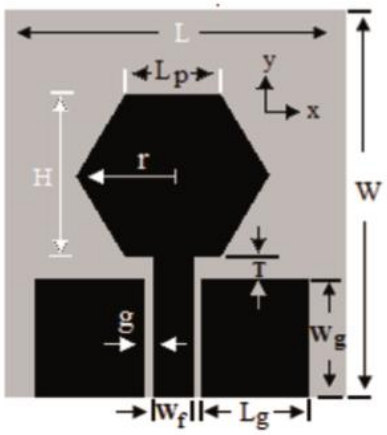

Figure 2.12: Hexagonal Shape for UWB Antenna

In Figure 2.13, the simulated gains are plotted against the frequencies which shows a visible drop at 3.5 GHz and 5.5 GHz.

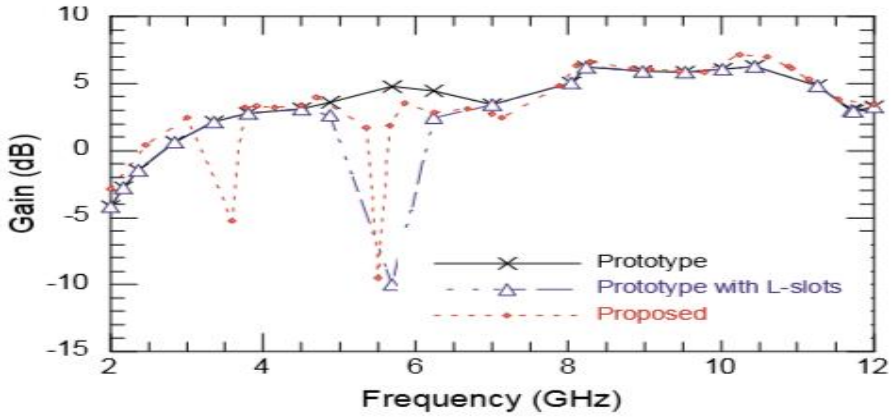

Figure 2.13: Gain versus Frequency plot

2.1.8 Octagonal Shape antenna

The foremost purpose of this design was to achieve a low radar cross-section. Minimum radar cross-section makes this sort of antenna difficult for the enemies to detect. The construction of this design is carried out in two parts. In the first part, a UWB antenna is designed which acts as the reference antenna. Subsequently, the reference antenna is modified in order to obtain the octagonal shaped UWB antenna with minimum radar cross-section. Metal surfaces are deleted in order to avoid minimum current distributions created by them [23].

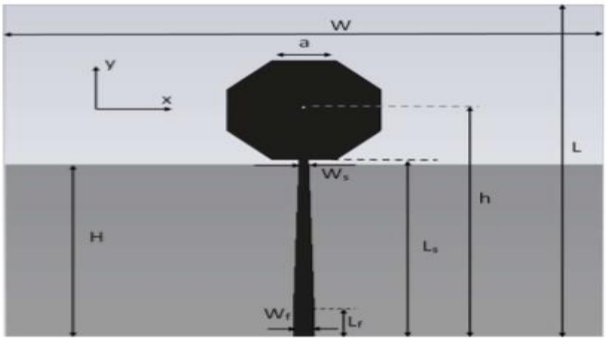

Figure 2.14: Octagonal Shaped UWB antenna

Figure 2.15 (a), (b) and (c) shows the radiation pattern obtained from this octagonal shaped UWB antenna at frequencies 3 GHz, 6 GHz and 13 GHz respectively.

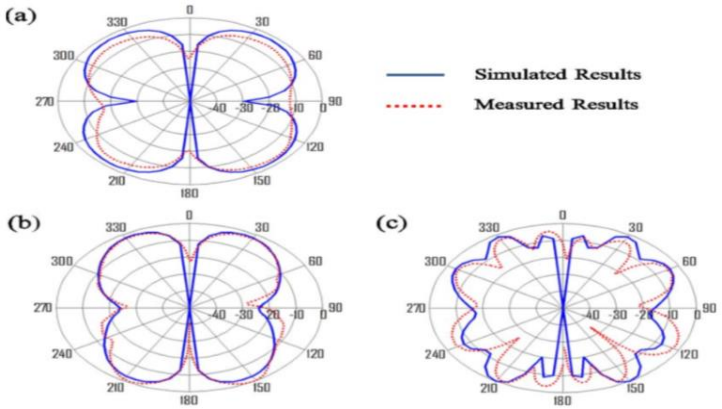

Figure 2.15: Radiation patterns of octagonal UWB antenna

2.1.9 Diamond Shape antenna

A Diamond shaped UWB antenna is designed for various applications. With the help of radiating patch which is diamond shaped and semi-circular ground plane, the bandwidth is greatly increased. The diamond shape radiating patch is obtained by applying a technique known as beveling technique. In this technique, a conventional rectangular antenna is used and the technique is applied to its corners in order to obtain a radiating patch. Because of the beveling of edges, smooth transition occurs between different modes resulting in bandwidth enhancement and improved impedance matching for a wide range of frequencies. Furthermore, microstrip feed line is used to fed the radiating element which additionally improves the impedance matching. Bandwidth enhancement along with improved impedance matching is achieved by replacing the conventional ground plane with a semi-circular ground plane [24].

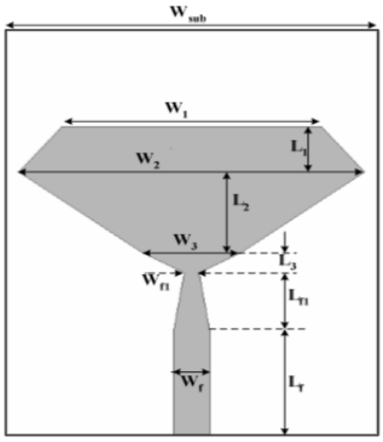

Figure 2.16: Diamond Shaped UWB antenna

Figure 2.17 shows the radiation pattern of the diamond shaped UWB antenna at 17.5 GHz

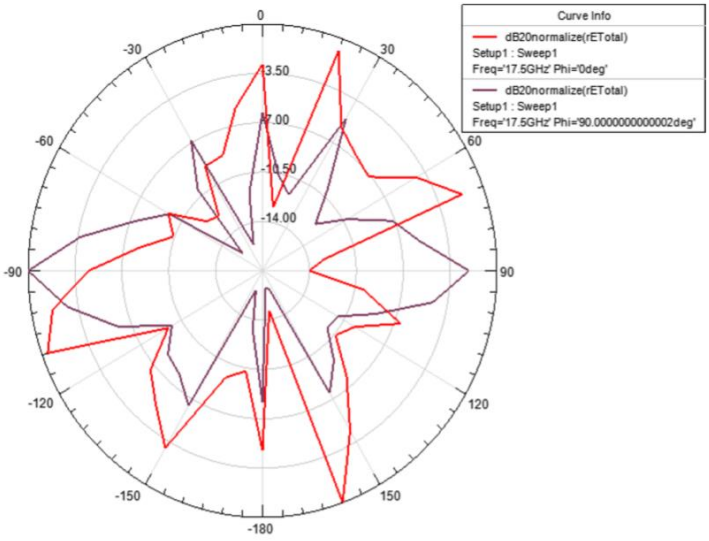

Figure 2.17: Radiation pattern at 17.5 GHz

2.1.10 Random Shape antenna

A printed UWB antenna that supports different mobile standards, such as DCS, PCS, UMTS and ISM bands is designed [25]. For the radiator, a spline-based representation is utilized and particle swarm optimization is utilized in order to obtain good impedance matching and stable radiation properties. Figure 2.18 depicts the shape of this antenna design.

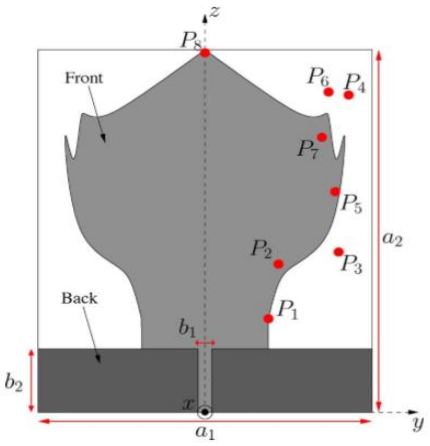

Figure 2.18: Random Shaped UWB Antenna

2.2 Frequency Selective Surface

Frequency Selective Surface (FSS) is a periodic, two- or three-dimensional array of elements etched on dielectric substrates. This array of elements could be patch type which acts as a band-stop filter or type of aperture which acts as a band-pass filter. Figure 2.19 shows the geometry of both these type of FSS elements i.e. patch type and FSS type.

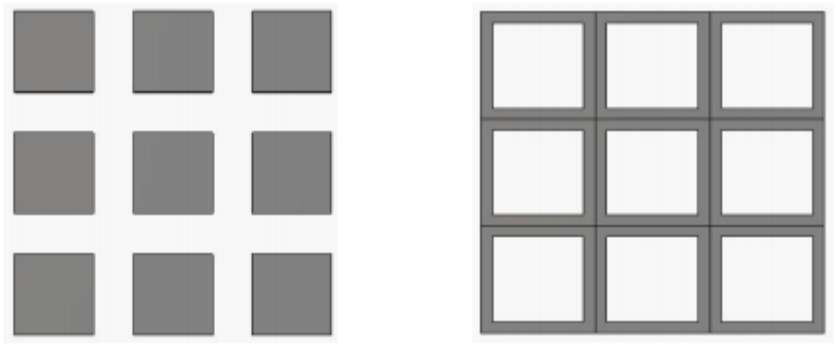

Figure 2.19: Geometries of patch and aperture type elements FSS array [26]

The literature presents various types of FSS element shapes, among which Jerusalem cross, simple straight dipole, square loop, circular loop, and the three legged dipole are the most common and are shown in Figure 2.20. Selective surfaces can monitor the transmission and reflection of electro-magnetic waves on the surface on the basis of physical structure and surface geometry frequency and function as band passes, low passes, band stops and high pass filters [26].

The FSS study is based on the diffraction gratings made in 1786 by David Rittenhouse an American physicist [27]. It was in the 1960s that extensive and groundbreaking research on selective frequency surfaces was performed. Frequency selective surfaces have spent more than five decades finding many applications in radar, communication and microwave systems.

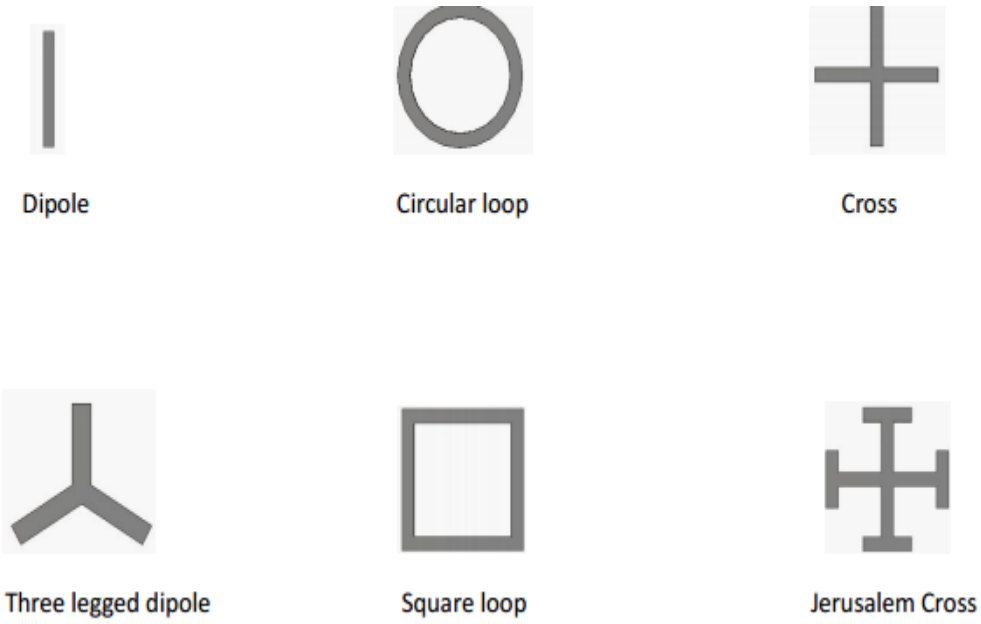

Figure 2.20: Unit cells of FSS element geometries [27]

Jerusalem cross is one of the oldest elements used for designing FSS. This form consists of two crossed dipoles having orthogonal sections at the ends as shown in Figure 2.20. This type of elements have a response of total reflection and compared to the tri-pole design, it shows better stability because of the shifting of incident angle from normal to 45 degrees in terms of bandwidth and harmonic[29].

2.2.1 Hexagonal elements

Patch type hexagonal FSS has a capacitive (low pass) response. These FSS elements have a stronger harmonic response [29].

2.2.1 Combination elements

A new design of FSS element can be obtained by combining the elements shown in Figure 2.20. This design forms another group of FSS elements which were named as

combinations by Munk. In this research, a combination of Jerusalem cross and hexagonal shaped element is presented. In literature, frequency selective surfaces (FSS) are also used as spatial filters. Researchers have done a lot of work aiming at transmitting and reflecting some of the frequency bands by the use of FSS. A key role is played by filters in various RF circuits for removing the unwanted signals and reducing the noise. On the basis of their behavior, filters can be classified into numerous types such as low pass, band pass, high pass and band stop filters. One of the important applications of FSS is radomes that are used to reduce the radar cross section of antennas [29]. As shown in Figure 2.21, various different types of FSS have different transmission behaviors and different surface impedances making it low pass, high pass, band pass and band stop etc.

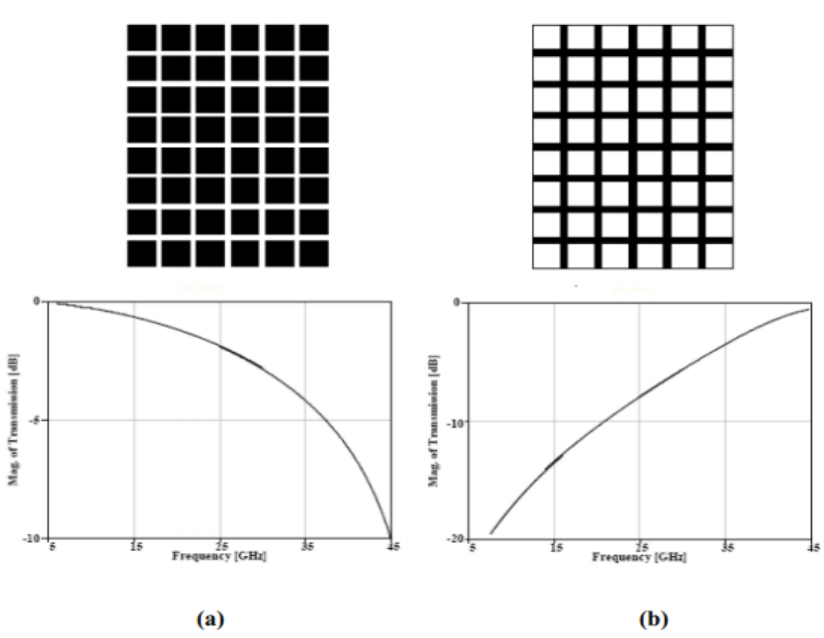

Figure 2.21: (a) Patch type and (b) slot type periodic structures with their surface impedance, the response of the patch array is capacitive and that of slot type is inductive [29]

From observation it is clear that there will be more reflection of electromagnetic waves from a surface with greater metal and the reflections from a surface with less metal will be weak. To see the actual scenario let us consider a metal surface in the form of long strips, and a metal surface in the form of short dipoles as shown in Figure 2.22. The long strip surface is supposed to produce large reflections than the small dipole surface but the study demonstrates that for certain frequencies, the small dipoles act as a total reflective surface. This was the problem investigated by Franklin and Marconi while introducing their reflector antenna [30] and the design for the periodic dipole elements is an inductor while that of the long strips array has an L-C circuit model. Thus the dipole array is fully reflective at the L-C circuit resonance frequency.

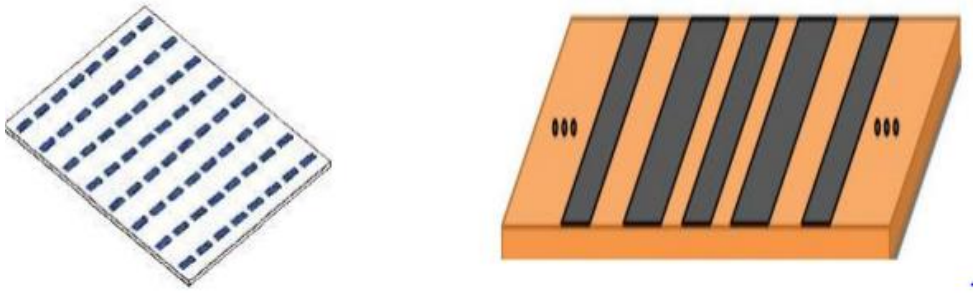

Figure 2.22: (a) Short dipole type FSS surface (b) Long strips type FSS surface

The basis of the FSS operating mechanism is on the resonant elements. As a plane wave illuminates the array of the metallic elements, the current becomes excited on the elements. Coupling of the energy concentration between the incident wave and the elements determines the intensity of the excited current. If the element's length is $\gamma/2$ then coupling will be at the maximum point at the fundamental frequency. Hence it is required to shape the elements in such a way that they resonate at the operational frequency. Current acts as an electromagnetic source, producing dispersed fields that depend on their distribution. The overall area covered by the FSS

consists of the accumulation of the dispersed field and the incident field. It therefore depends on the design of the element to produce the required filter response and the frequency behavior of the selective frequency surfaces is ascertained by the current distribution on the elements.

Given that the FSS frequency response is critically affected by the geometry of the FSS elements discussed above, there are several other parameters that also affect the FSS frequency response such as the type of substrate used and the inter-element spacing. The substrate material used affects both the bandwidth and the operating frequency while the inter-element spacing on the other hand raises the issue of the grating lob. The onset of the grating lob will be earlier if the inter-element space is large so that small spacing between the elements is more appropriate to avoid the problem of grating lob. Inter-element spacing also has affect on the bandwidth, smaller the space, larger will be the bandwidth [31].

The most optimal way to characterize selective frequency surfaces is by its scattering parameters [32]. Frequency selective surface being a two-dimensional array describes the operational scenario by dividing the entire free space into two areas, one containing the source of the electromagnetic waves and the other containing the remainder space. The reflection and transmission of energy off the FSS surface and through the FSS surface respectively give the solution for the wave propagation into the space. If anyone is provided with these coefficients of reflection and transmission he may easily explain the interaction between the source and the FSS layer. There are numerically different techniques available in the literature [20]-[26] in order to analyze the FSS layer but this is not the concern of this thesis. A few methods are defined in [25]-[27] to calculate the coefficients of transmission and reflection.

2.3 Radar Cross Section (RCS) Reduction

2.3.1 Planar Octagonal-Shaped UWB Antenna

In this research work, a novel planar octagonal-shaped antenna with reduced radar cross section (RCS) is designed and experimentally demonstrated for ultra-wideband (UWB) applications. To get the RCS reduction, the proposed antenna is modified using the geometrical shaping method. This method is based on the subtraction of metal areas on the surface of the printed antenna which have the minimum currents distributions. The full-wave electromagnetic simulations and laboratory measurements are carried out to classify their RCS as a function of frequency, radiation patterns, and scattering characteristics. The radiation performance of modified antenna is stable and consistent with the reference antenna. The results also show that the built UWB antenna has lower RCS over the reference antenna. RCS reduction of about 10 dBsm is obtained throughout the entire operation bandwidth. The antenna designed has very large RCS reduction of up to 25 dBsm, particularly in the low frequency range [33].

The designed bandwidth of the UWB antenna is 2.5–18 GHz which covers the entire band assigned for UWB applications. To minimize antenna RCS, the designed UWB antenna was modified by geometrical shaping. The validation of bandwidth and radiation properties of both the modifies antenna and the reference antenna were validated via EM simulations and measured results for the manufactured antennas. The results show that according to the reference antenna the modified antenna has almost the same radiation pattern, return loss and gain characteristics. Additionally, both EM simulations and measurements have verified the backscattering characteristics of the antennas. The designed UWB antenna has lower RCS throughout the entire operating bandwidth, particularly in the low frequency range compared with the reference antenna. Also for oblique incident waves, the modified antenna has lower RCS value. All of

these results for the proposed antenna are evidence that it can be conveniently used as a UWB antenna where the low RCS is desired.

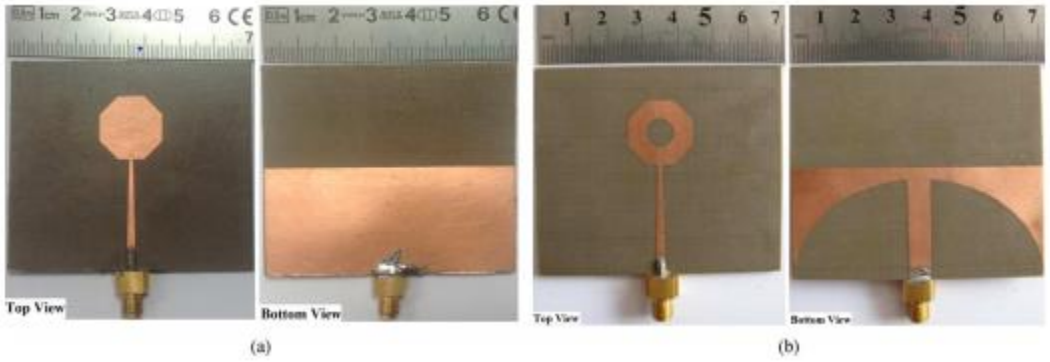

Figure 2.23: Octagonal-shaped UWB antennas (a) Reference (b) Modified

2.3.2 Low RCS Micro-strip Patch Antenna Using Frequency-Selective Surface and Micro-strip Resonator

This design proposed in this paper is based on implementing frequency-selective surfaces (FSSs) and micro-strip resonators. Out of band RCS reduction can be realized by using the FSS ground instead of the solid metal ground. In addition, in-band RCS reduction can be achieved by loading micro-strip resonators. A significant reduction of the RCS in the frequency ranges of 3-10 GHz has been achieved. The simulation results show that the RCS reduction of the proposed antenna in and out of the operating band is as much as 13 and 17 dB , respectively, compared with the reference antenna. Measured results are satisfyingly in accordance with the simulated tests. The radiation performance of the proposed antenna is conserved compared to the reference antenna [34]. The results show that wideband RCS reduction can be acquired by combining FSSs and micro-strip resonators on the evidence of acceptable detrimental effect on the radiation properties. Excellent RCS reduction in 3–10 GHz frequency ranges is implemented

at the cost of a slight resonant or frequency shift and a low loss of gain. Therefore, the antenna can be used in low-RCS platforms, with these outstanding features.

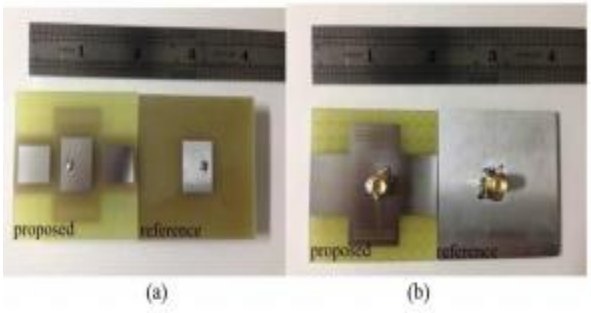

Figure 2.24: (a) Top and (b) bottom view of two fabricated antennas

2.3.3 Wideband radar cross-section reduction of micro-strip patch antenna with split-ring resonators

A novel technique for the reduction of radar cross-section (RCS) for a wideband micro-strip antenna along with preserving its radiating performance, is proposed and investigated. The design idea is based on substituting the solid metal ground with the hybrid ground, which is composed of appropriate compact split-ring resonators. The antenna which is irradiated in the normal direction by transverse-electric and transverse-magnetic polarized waves is examined and investigated. Results demonstrate that RCS is decreased dramatically over a broad frequency range from 2 to 20 GHz. By comparison, the proposed strategy can obtain remarkable RCS reduction of around 11 dB at 20 GHz. The superior performance and reliability of the proposed design are demonstrated on the basis of the acceptable effect on radiation features and prominent reduction of RCS [35].

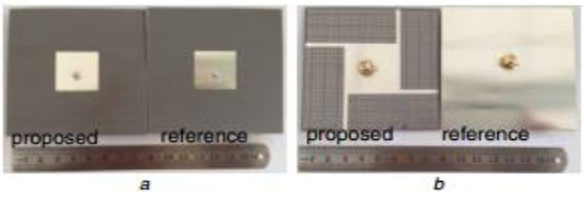

Figure 2.25: Reference and proposed antennas a)Top view b) Bottom view

2.3.4 Ultra Wideband Antenna with Reduced Radar Cross Section

In this work, an octagonal ultra wideband antenna with reduced RCS has been proposed. The proposed antenna functions in the 3.6GHz to 16GHz frequency range with an impedance bandwidth of more than 115%. The antenna has been optimized with improved RCS of almost 50 % (without affecting the overall performance) than previously stated works. The reduction of RCS is accomplished in a wide frequency band covering the antenna's wide operating band by subtracting metal areas which have the minimum current distributions on the printed antenna surface. Measured results were in line with the simulated values. The proposed antenna is a good candidate for application requiring operation of UWB with low RCS [36].

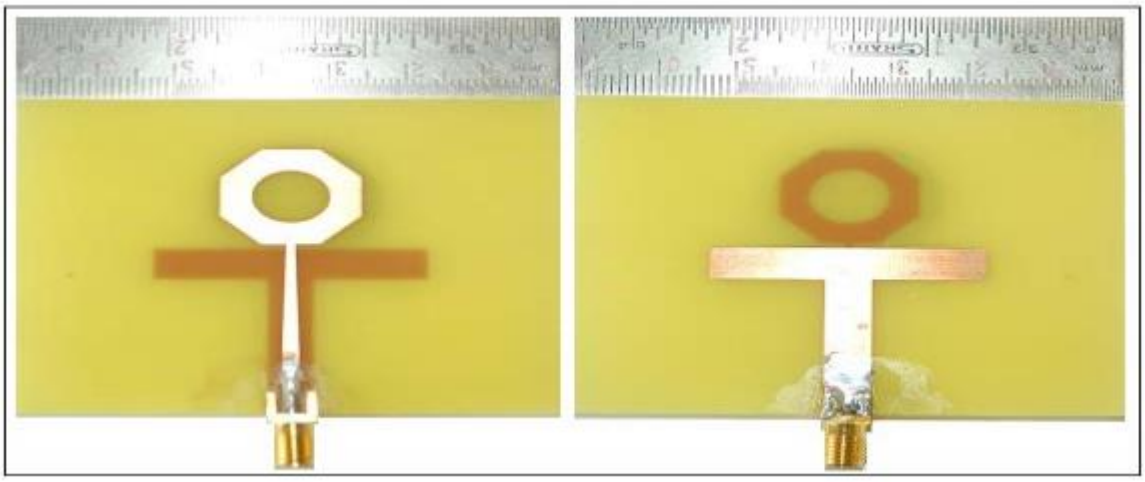

Figure 2.26: Fabricated prototypes Top view (left) and bottom view (right)

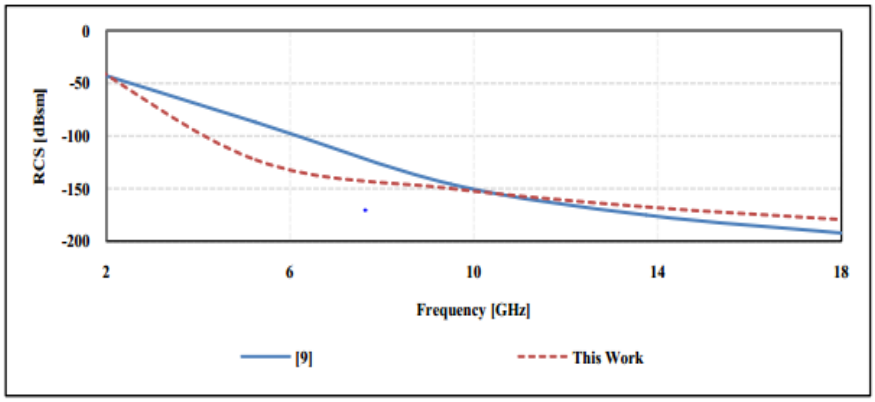

Figure 2.27: Simulation results of mono-static RCS for x-polarized incident wave impinging from normal direction

2.3.5 Radar Cross Section Reduction of a Micro-strip Antenna Based on Polarization Conversion Meta-material

The PCM based micro-strip patch antenna has been simulated and measured to prove to be a great trade-off between RCSR and radiating properties. It was seen that a remarkable RCSR can be obtained by properly designing periodic PCM that is placed around the radiating patch. On the basis of unobvious effect on the antenna performance, noticeable in-band and out-of-band RCSR make the strategy a good candidate for the design of antennas on a low-observability platform [37].

Figure 2.28: Reference and proposed antennas: (a) top view (b) bottom view

2.3.6 Gain Enhancement and RCS Reduction for Patch Antenna by Using Polarization Dependent EBG Surface

A novel antenna incorporated with polarization-dependent EBG structure is proposed in this letter for design of high-gain and low-RCS antennas. Because of its controllable induced currents, a slot type of EBG is adopted, and the gain enhancement mechanism by the EBGs is clearly explained. Some EBG components are used to improve the radiation depending on the function, and the rest form a chessboard reflector to reduce the scatterings of the whole antenna. Chess-board fine details are modified to offset the deformation caused by the radiation elements. The simulation and measurement results show that the proposed antenna achieves gain enhancement of 2.5 dB and RCS reduction of more than 4.3 dB for normal incidence simultaneously, compared with the traditional patch antenna [38].

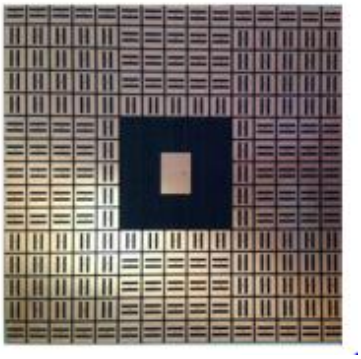

Figure 2.29: Photograph of fabricated slot-EBG antenna prototype

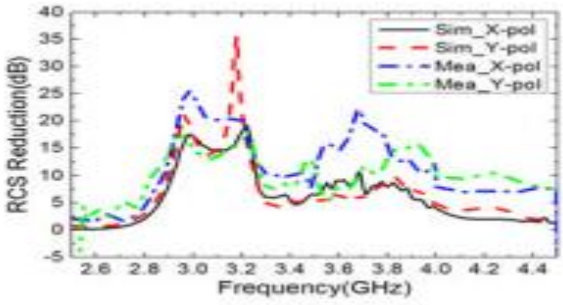

Figure 2.30: Simulated and measured RCS reduction versus frequency forx-andy-polarization plane waves

2.3.7 Radar Cross Section Reduction of Micro-strip Antenna Using Dual-Band Meta-material Absorber

In this work, a dual-band meta-material radar absorbing structure for the reduction of radar cross section (RCS) of a micro-strip antenna is designed and verified experimentally. A Metamaterial Absorber (MMA) is designed to operate at an absorption rate of approximately 100% in X-band. Its impact on RCS and efficiency of a micro-strip antenna is investigated in order to demonstrate the successful performance of the proposed structure. Based on the numerical and measurement results, the designed antenna shows dual-band RCS reduction within X-band for wide incident angles, whereas the radiation characteristics of antenna are maintained without undesirable changes. The numerical and experimental results show that dual-band RCS reduction can be obtained by combining micro-strip antennas with MMAs. Meanwhile, micro-strip antenna performance is conserved when using the MMA. The measured results show that the antenna obtains a reduction of 20 and 10 dB RCS almost at 8.5 and 11.2 GHz, while its out-band radiation efficiency is maintained favorably [39].

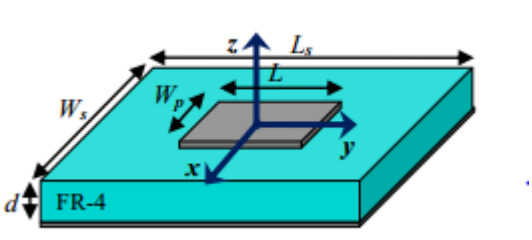

Figure 2.31: Micro-strip antenna with dimensions of:Lp = 14.6 mm,Wp = 10.6 mm, Ls = 52.5 mm, Ws = 52.5 mm, l4 = 2.9 mm,and d = 0.8 mm

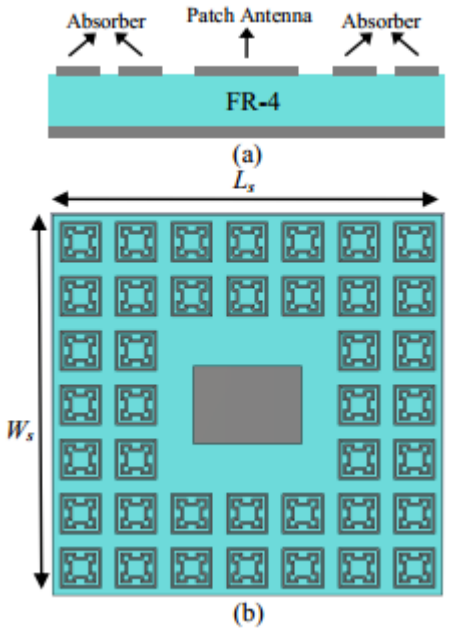

Figure 2.32: Configuration of low RCS micro-strip antenna (a) Side view and (b) top view

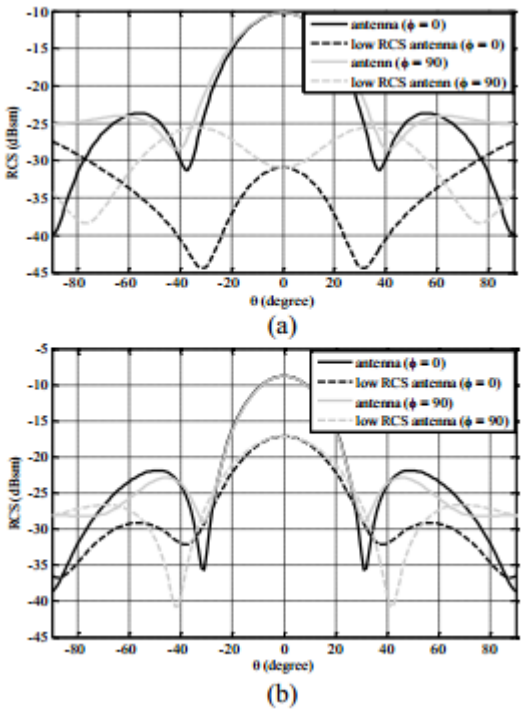

Figure 2.33: Simulated mono-static RCS of micro-strip antenna with and without absorber at under normal incidence at: (a) 8.4 and (b) 11.1 GHz

2.3.8 In-Band RCS Reduction and Gain Enhancement of a Dual-Band PRMS-Antenna

The in-band RCS reduction and gain enhancement of a dual-band PRMS-antenna was obtained in this letter after loading a reference patch to a planar-modified PRMS checkerboard configuration. In order to validate the radiation and scatter performance of the proposed antenna, numerical simulations and experimental measurements have been used. Both the simulation and measurements are in well agreement. The dual-band PRMS-antenna design provides with a novel method for reducing the contribution of antenna in the overall RCS by synthetically decreasing the number and RCS of antennas [40].

Figure 2.34: Fabrication of the proposed antenna

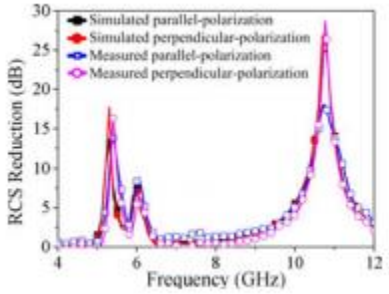

Figure 2.35: Measurement results of RCS reduction for both polarizations under normal direction

2.3.9 Broadband RCS Reduction of Micro-strip Antenna Using Coding Frequency Selective Surface

A novel RCSR method is proposed which is established on the basis of FSS coding by developing an optimization algorithm using CST software as the computational core of the algorithm. Simulation and measured results indicate that the RCS of the proposed antenna is considerably reduced by up to 12dB in the entire X-band, and that the maximum RCS reduction is achieved at a frequency of 8.8 GHz at almost 24 dB. Furthermore, the reduction of 10-dB RCS is found from 6.25 GHz to 12 GHz (63%) [41].

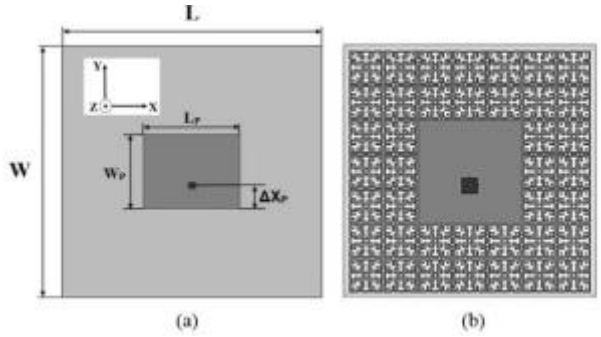

Figure 2.36: Low RCS Antenna using one bit coding FSS in ground plane. (a) Top view. (b) Bottom view

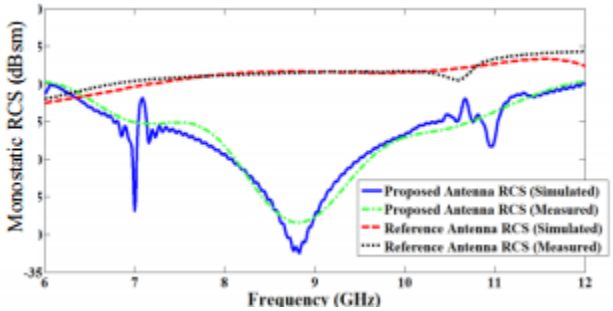

Figure 2.37: Comparison of mono-static RCS between measured and simulated of the reference and proposed antennas in the frequency range of 6 GHz-12 GHz

Chapter 3

Simulation of UWB Antenna with FSS

In this chapter, the design and analysis of patch antenna with the reduce radar cross section (RCS) has been discussed. The proposed antenna with FSS structure has been simulated in high frequency structure simulator (HFSS) and results has been presented. The design process of this antenna is divided into three parts. First part includes the design of a single element micro-strip patch antenna. Second part includes the design of the FSS unit cell and FSS array. In third stage, the design of patch antenna with FSS at a separation distance of 4 mm. The aim of this design process is to come up with a patch antenna with reduced RCS it terms of enhancing the gain of the antenna.

3.1 UWB Antenna

There is an increased interest in ultra-wideband (UWB) technology for it's widespread use in several present and future applications. UWB technology received a major boost especially in 2002 since the US Federal Communication Commission (FCC) permitted the authorization of using the unlicensed frequency band starting from 3.1 to 10.6 GHz for commercial communication applications [1]. This large bandwidth spectrum is available for high data rate communications as well as radar and safety applications to operate in. The UWB technology has another advantage from the power consumption point of view. Due to spreading the energy of the UWB signals over a large frequency band, the maximum power available to the antenna as part of UWB system will be as small as in order of 0.5 mW according to the FCC

spectral mask [2]. This power is considered to be a small value and it is actually very close to the noise floor compared to what is currently used in different radio communication systems.

With the increasing popularity of UWB systems, there have been breakthroughs in the design of UWB antennas. Implementation of a UWB system is facing many challenges and one of these challenges is to develop an appropriate antenna. This is because the antenna is an important part of the UWB system and it affects the overall performance of the system.

Currently, there are many antenna designs that can achieve broad bandwidth to be used in UWB systems. Due to their wide frequency impedance bandwidth, simple structure, easy to fabricate on printed circuit boards (PCBs), and omnidirectional radiation patterns, printed PCB versions of planar monopole antennas are considered to be promising candidates for applications in UWB communications. Recent UWB antenna designs focus on small printed antennas because of their ease of fabrication and their ability to be integrated with other components on the same PCBs [40].

3.2 Antenna for Ku/K band Applications

The increasing demand for the frequencies has led to the appearance of several frequency bands, among them is Ku band. It is the most used of all the frequency bands for satellite communication systems. It is conventionally defined in the electromagnetic spectrum defined by the microwave frequency band from 12.4 GHz to 18 GHz. This band is the most widespread in the world because of compactness.

3.2.1 Parametric Study

The design process of any antenna starts with the selection of the dielectric substrate depending upon the antenna's requirement. In this case FR4 is selected as a substrate. FR4 has dielectric constant value of 4.4, thickness of 1 mm and loss tangent of 0.02. Reason behind the selection of FR4 is its ease of availability in market, low cost and it can be easily fabricated in any shape. The goal of this design is to achieve overall impedance bandwidth of wide range while keeping an antenna size small and obtaining the reduced radar cross section while enhancing the gain of the antenna. For designing antenna the required dimensions of antenna patch, ground and substrate are calculated by carrying the following steps:

Step 1: Calculation of the Width.

$$W = \frac{c}{2f_0\sqrt{\frac{\varepsilon_r+1}{2}}}.$$

(1)

Step 2: Calculation of the Effective Dielectric Constant. This is based on the height, dielectric constant of the dielectric and the calculated width of the patch antenna

$$\in_{eff} = \frac{\varepsilon_r+1}{2} + \frac{\varepsilon_r-1}{2}\left[1 + 12\frac{h}{w}\right]^{-\frac{1}{2}}.$$

(2)

Step 3: Calculation of the Effective length.

$$\mathrm{L_{eff}} = \frac{\mathrm{c}}{2\mathrm{f_0}\sqrt{\varepsilon_{\mathrm{eff}}}}.$$

(3)

Step 4: Calculation of the length extension ΔL.

$$\Delta L = 0.412h\frac{(\varepsilon_{eff})\left(\frac{w}{h}+0.264\right)}{(\varepsilon_{eff}-0.258)\left(\frac{w}{h}+0.8\right)}.$$

(4)

Step 5: Calculation of actual length of the patch.

$$L = L_{eff} - 2\Delta L$$

(5)

where, the following parameters are used

f_0 is the Resonance Frequency.

W is the width of the Patch.

L is the Length of the Patch.

h is the thickness.

εr is the relative Permittivity of the dielectric substrate.

c is the Speed of light: 3 x 10^8m/s.

3.2.2 Analytical Design

As Ultra Wide Band (UWB) covers 3.1-10.6 Ghz frequency band, so the resonant frequency of the antenna should be the central frequency that is 5.7Ghz. All the antenna calculations are done on the central frequency, the optimization of different parameters are done to get better results. In previous chapter it is discussed that monopole antennas have dual benefits as its offers larger impedance bandwidth as well as size compactness. Monopole antennas consist of three parts which includes radiation patch, ground plane and a feed line. Partial ground plays a major role to get whole coverage of UWB band. The design of antenna starts with selection of shape and calculation of dimensions of antenna.

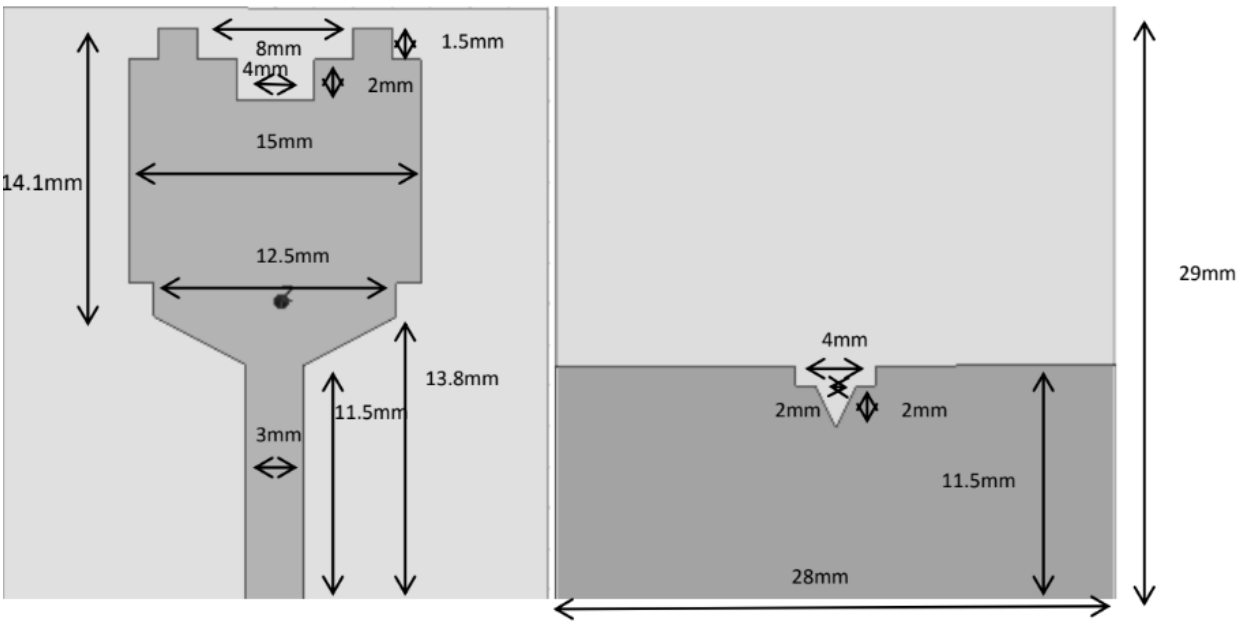

(a) (b)

Figure 3.1 UWB Antenna (a) front view (b) back view

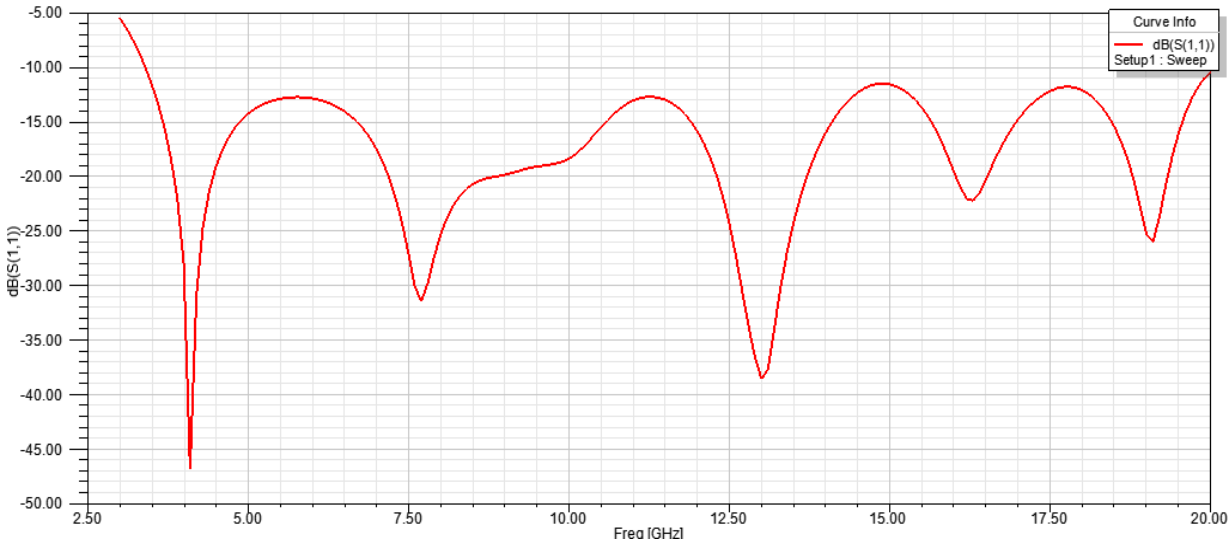

Figure 3.2 Reflection of UWB antenna

Rectangular patch is selected as a radiating element of monopole antenna and the dimension are 16.5 ×15 mm^2. The size of radiation patch of antenna tells us about the overall size of the antenna. For the impedance matching of a patch antenna with 50Ω SMA connector

fed length transmission line is 11.5 mm and width of 3 mm. Patch is tapering from ground having distance 3 mm. To get UWB result stair case technique describe previous chapter is used to get results. Ground of antenna is also modified. So result of S11 is cover band 3.3-20 GHz [41].

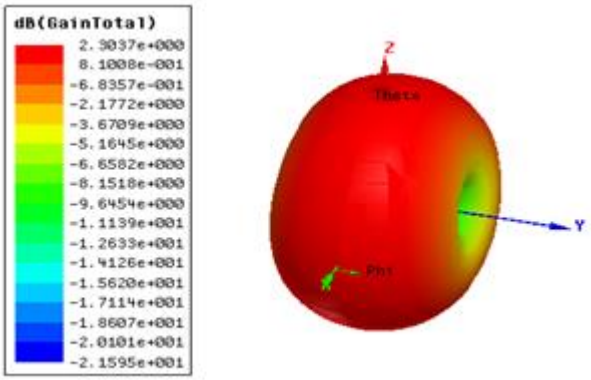

Figure 3.3 3D Gain Plot of UWB antenna at 5.7 GHz

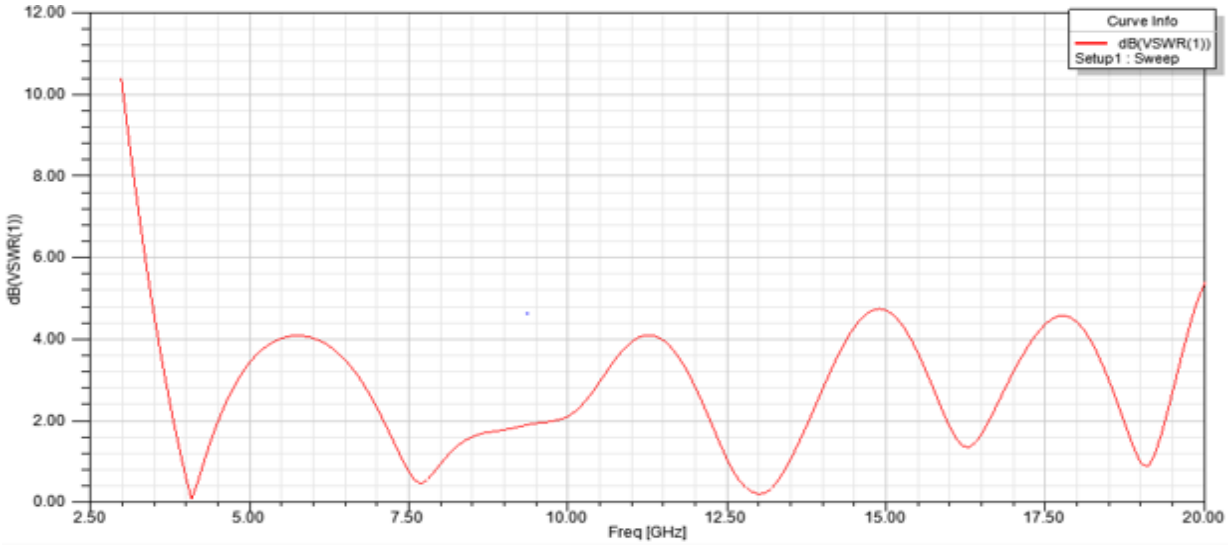

Figure 3.4 VSWR of UWB antenna

For UWB micro-strip patch antenna the s11 should be less than -10dB. After the simulation of antenna on HFSS the graph clearly shows from 3GHz to 20 GHz the s11 is less

than -10dB. So overall antenna design fulfills the condition of UWB requirement. As well as the antenna covers 10GHz additional so this design cover 130% more band. So the design can be considered as an effective one in terms of s11.The antenna s11 results shows that it is also giving good results up to 20 GHz so the antenna has an application for the K/Ku band.

Voltage standing wave ratio (VSWR) of the antenna is shown in the Fig 3.4 the VSWR value for the good antenna design should be less than 2 and the figure above shows that the value of VSWR < 2 at multiple frequencies.

3.2.3 Design of FSS

FSS is a periodic surface with identical two-dimensional arrays of elements arranged on a dielectric substrate. An incoming plane wave will either be transmitted (pass band) or reflected back (stop band), completely or partially, depending on the nature of array elements. This occurs when the frequency of electromagnetic (EM) wave matches with the resonant frequency of the FSS elements. Therefore, an FSS is capable of passing or blocking the EM waves of certain range of frequencies in the free space; consequently, identified as spatial filters. Nowadays, FSSs have been studied comprehensively and huge growth is perceived in the field of its designing and implementation for different practical applications at frequency ranges of microwave to optical.

Step-1: Unit Cell Design

The unit cell of the FSS consists of an array of conducting patches printed on one side of the dielectric substrate material Rogers 5880 having relative permittivity 2.2 and a thickness of 1.588 mm. The shape and dimensions of the unit cell is illustrated in Fig.3.5.

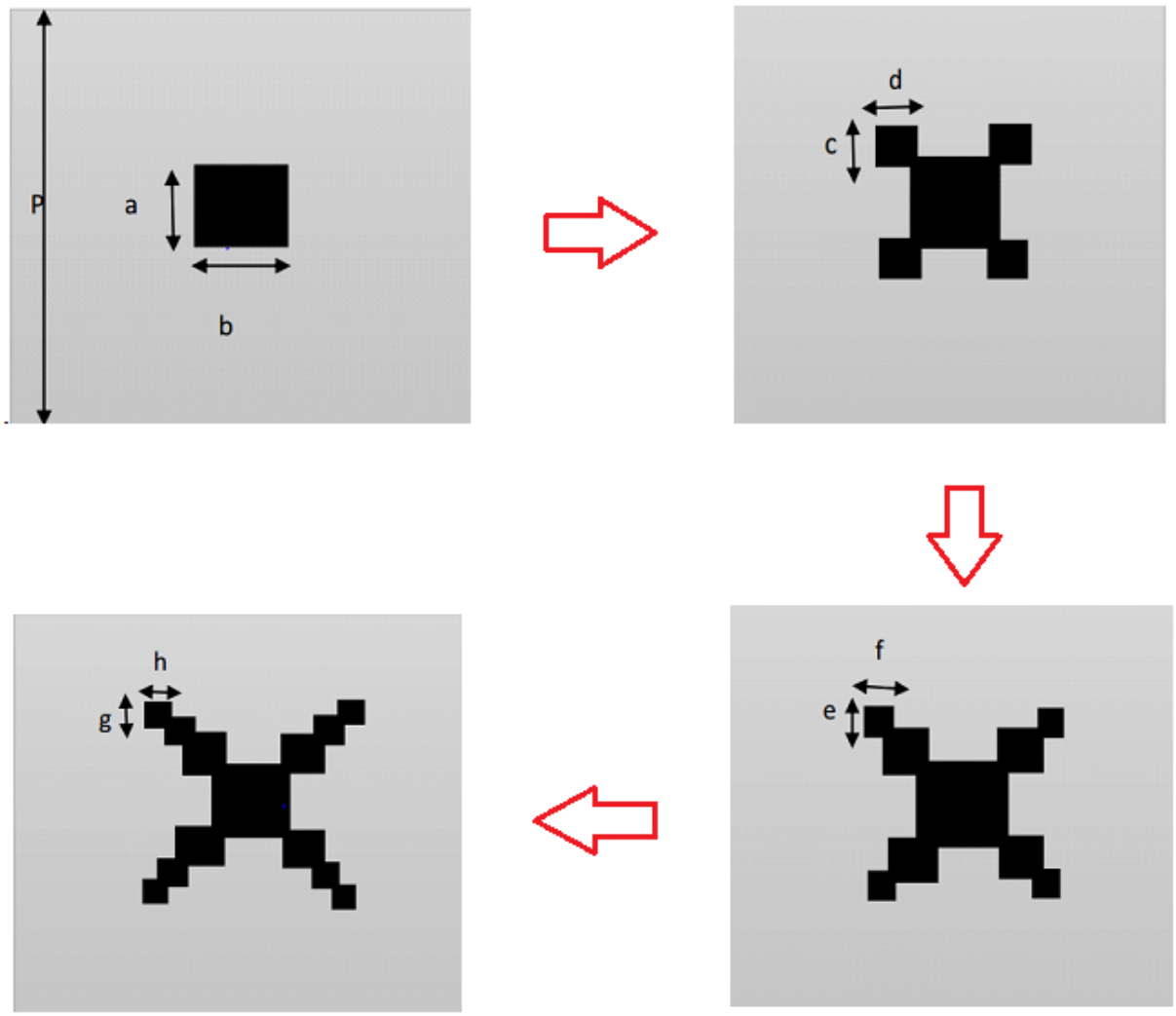

Figure 3.5 Design of unit cell with parameters (a=b=2.25mm, c=d=1.5mm, e=f=0.75mm, g=h=0.75mm, p=7.5mm)

The frequency characteristics of the unit cell of FSS are analyzed by using the HFSS 13, for the analysis of frequency Selective Surfaces and other periodic structures such as planner phased array floquet ports are used. The periodic structures are considered to be infinitely large and are analyzed by just analyzing their unit cell. The basic requirements for floquet port analysis are the linked boundaries of the unit cell walls, boundary conditions are such that they are infinitely spaced and for the excitations of the unit cell we need two floquet ports one for the top and other for the bottom. The floquet port have fields at the port boundaries otherwise the

mechanism is same as the Wave port where the perfect electric and magnetic conductors are assigned to all the boundaries of the unit cell box.

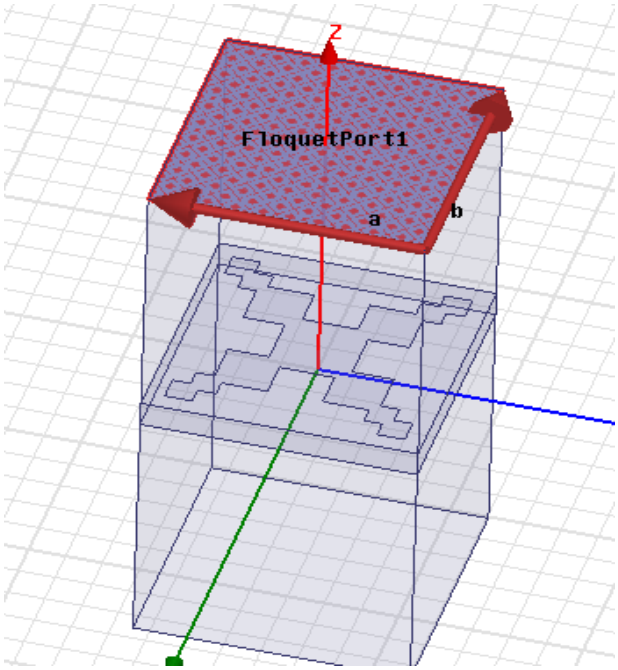

Figure 3.6 Unit cell with Floquet ports assigned

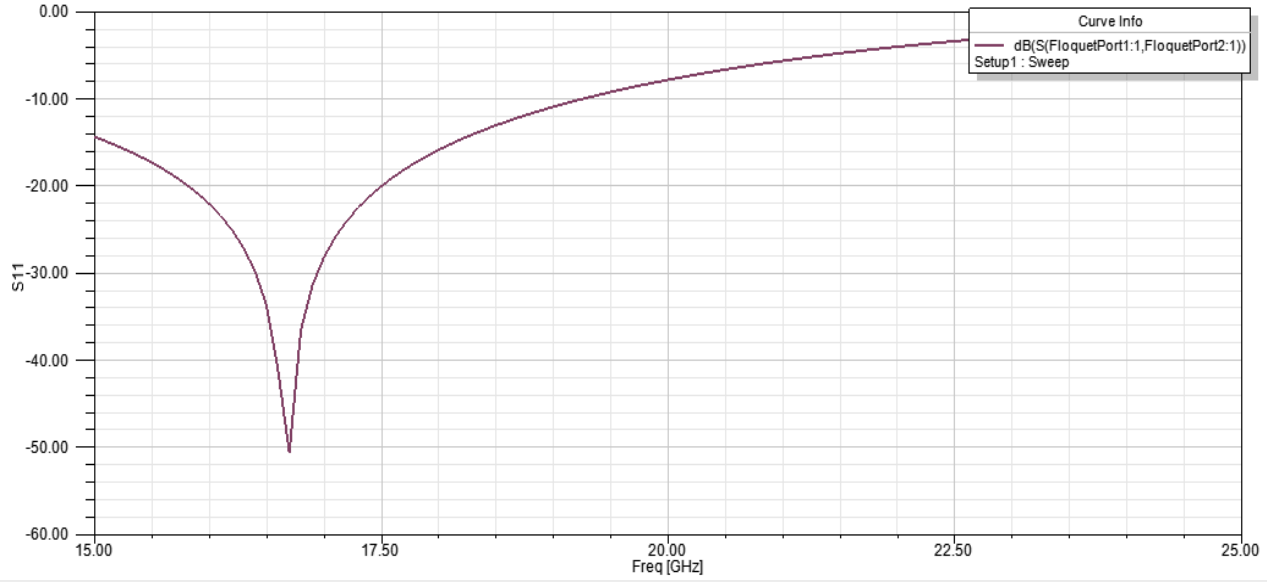

Figure 3.7 Reflection coefficient of single unit cell

The s-parameters shows that the unit cell is giving return loss of -50 dB at the frequency of 16.75GHz which is good enough for making it work with the antenna.

Step-2: FSS Array Design

The two dimensional array structure of the FSS is illustrated in Fig. 3.5. The structure has been simulated in HFSS and RT/Duroid 5880 substrate has been used. The separation distance between two elements is 1.5 mm.

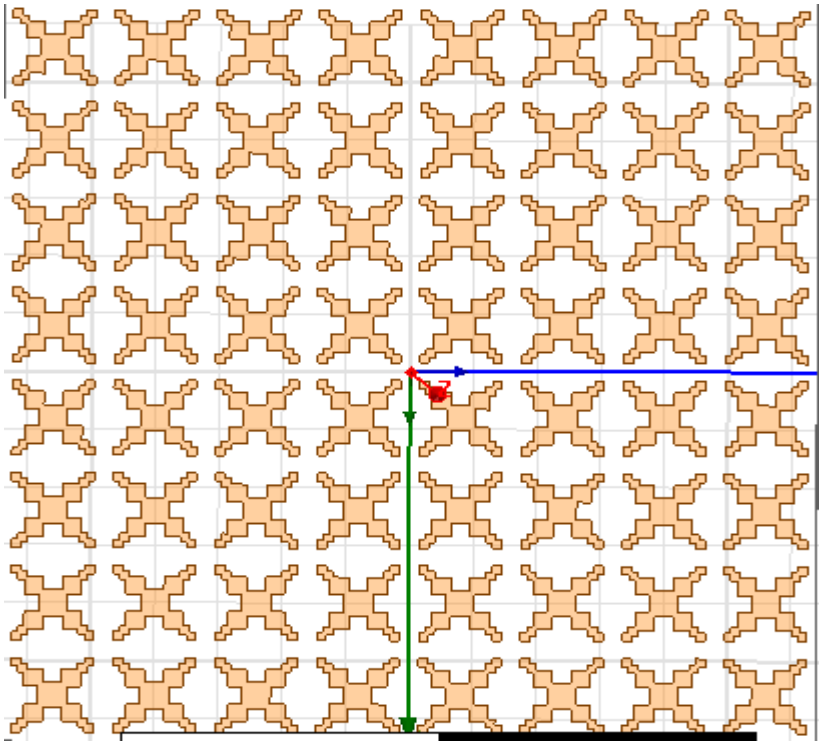

Figure 3.8 Frequency selective surface (FSS) 8×8 array

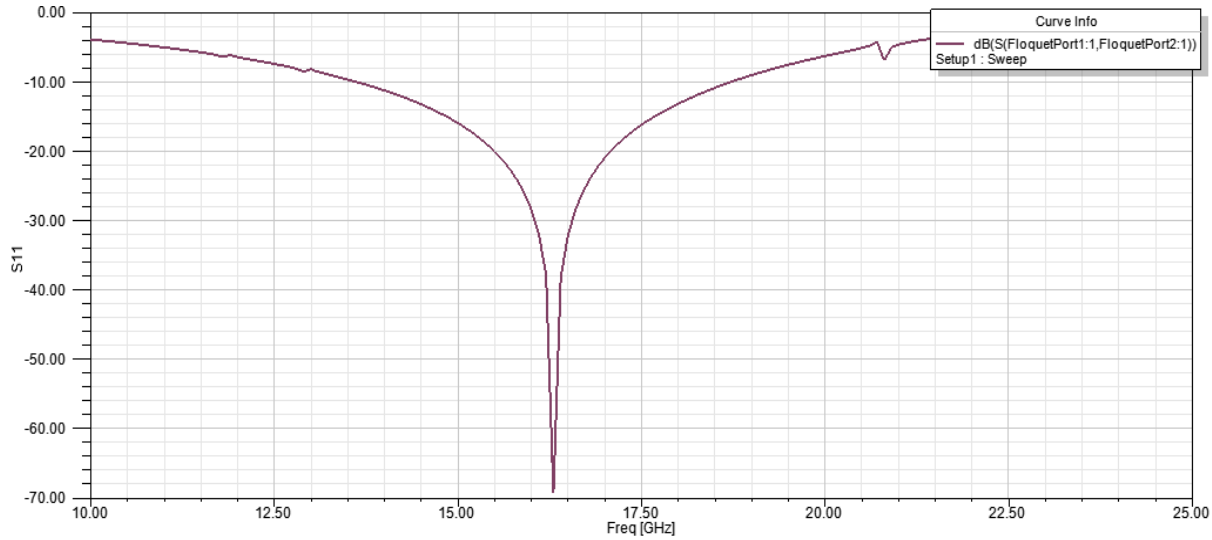

Figure 3.9 Reflection coefficient of FSS array

3.2.4 Antenna with FSS

Micro-strip patch antenna model consists of a radiating source and FSS layer placed above the

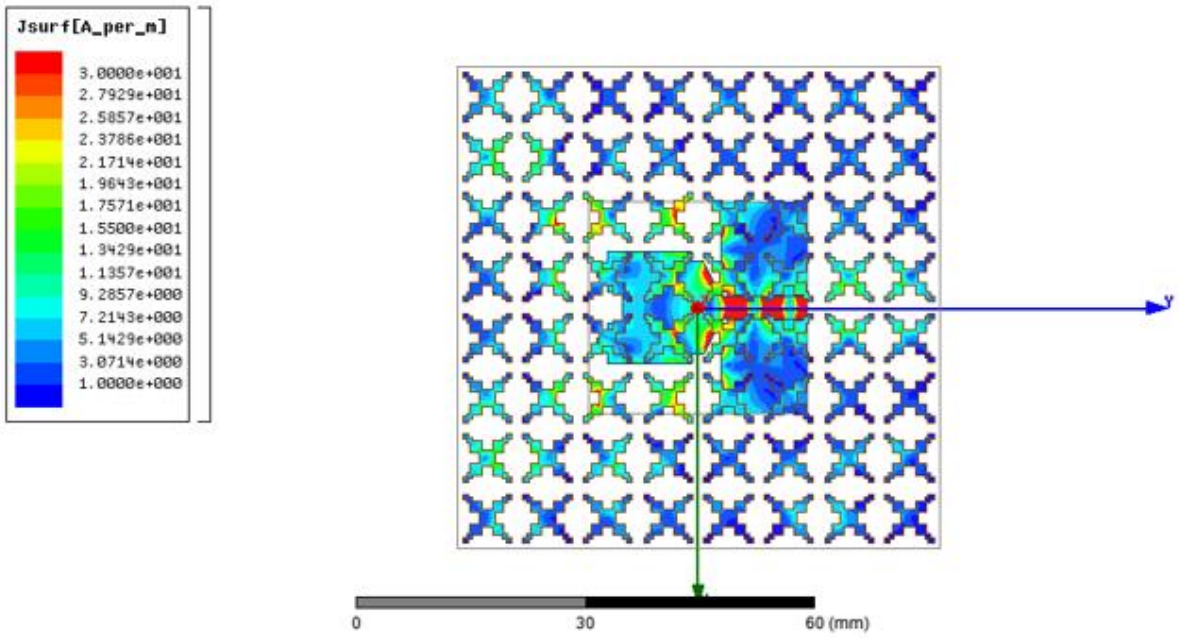

Figure 3.10 8×8 patch antenna with FSS array

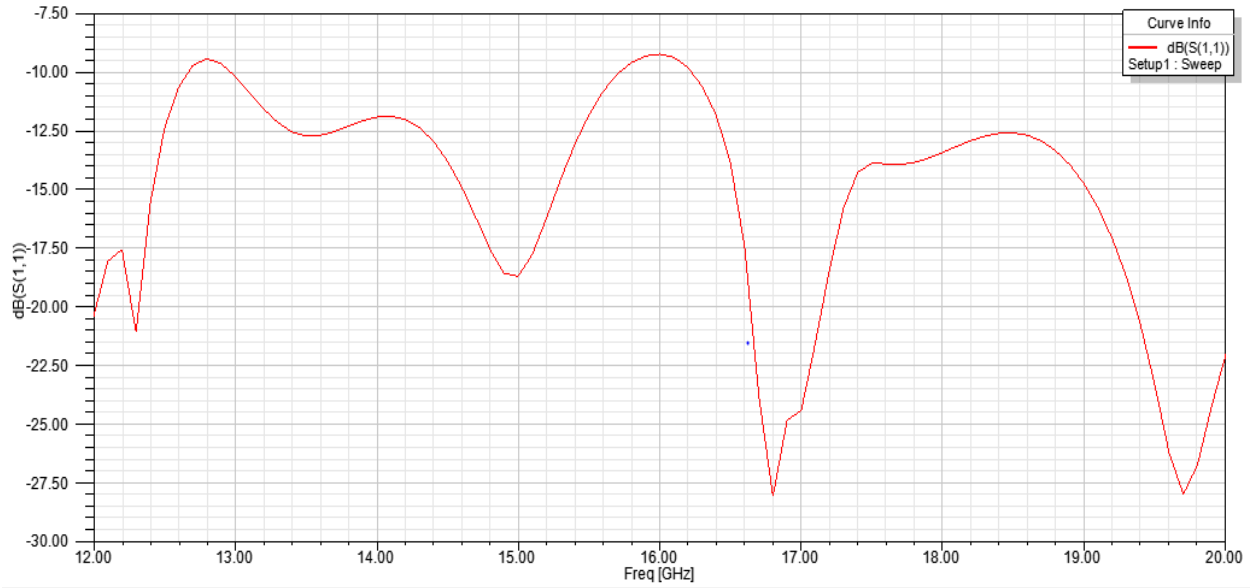

Figure 3.11 S-Parameters of antenna with FSS

The 3D gain plot is calculated by placing the FSS at different heights from the antenna and the gain plot for different heights are shown below.

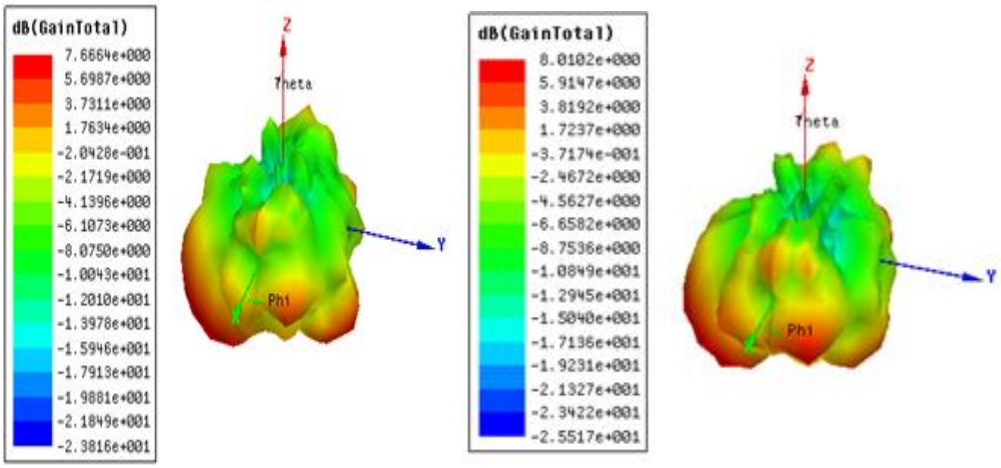

(a) (b)

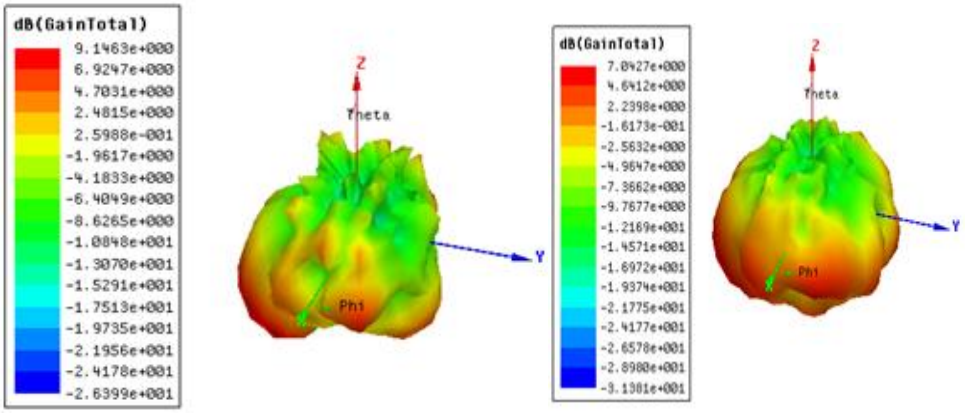

(c) (d)

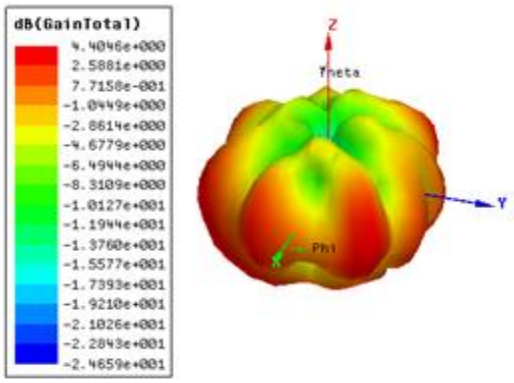

(e)

Figure 3.12 3D Gain plot for antenna with FSS at different heights (a) 2mm (b) 3mm (c) 4mm (d) 5mm (e) 6mm

From the above plots it can be noted that the ideal distance between the antenna and FSS is considered to be 4mm because it is giving the maximum value of gain at this distance i.e; 9.146 dB. So, all the calculations are done at the distance of 4mm.

The 3D Gain plots at different frequencies are shown in the figure 3.13

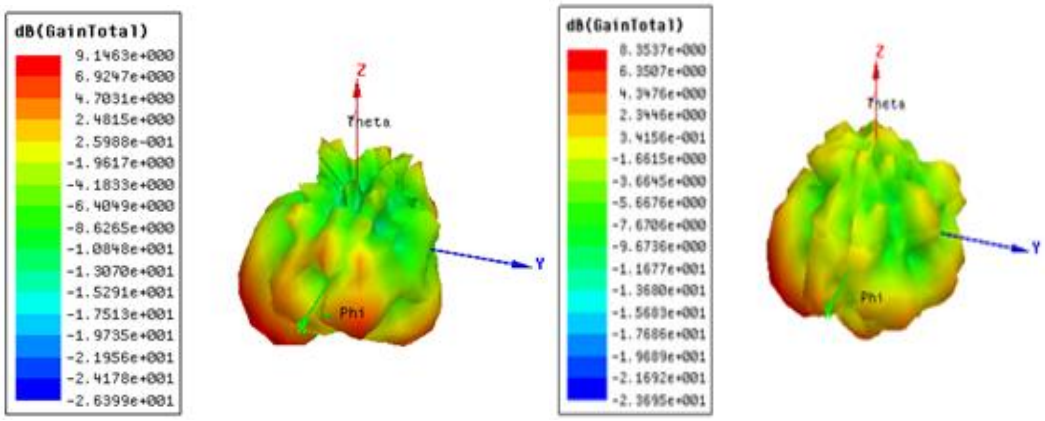
dB(GainTotal)
9.1463e+000
6.9247e+000
4.7031e+000
2.4815e+000
2.5988e-001
-1.9617e+000
-4.1833e+000
-6.4049e+000
-8.6265e+000
-1.0848e+001
-1.3070e+001
-1.5291e+001
-1.7513e+001
-1.9735e+001
-2.1956e+001
-2.4178e+001
-2.6399e+001
Z
Theta
Y
Phi
dB(GainTotal)
8.3537e+000
6.3507e+000
4.3476e+000
2.3446e+000
3.4156e-001
-1.6615e+000
-3.6645e+000
-5.6676e+000
-7.6706e+000
-9.6736e+000
-1.1677e+001
-1.3680e+001
-1.5683e+001
-1.7686e+001
-1.9689e+001
-2.1692e+001
-2.3695e+001
Z
Theta
Y
Phi

(a) (b)

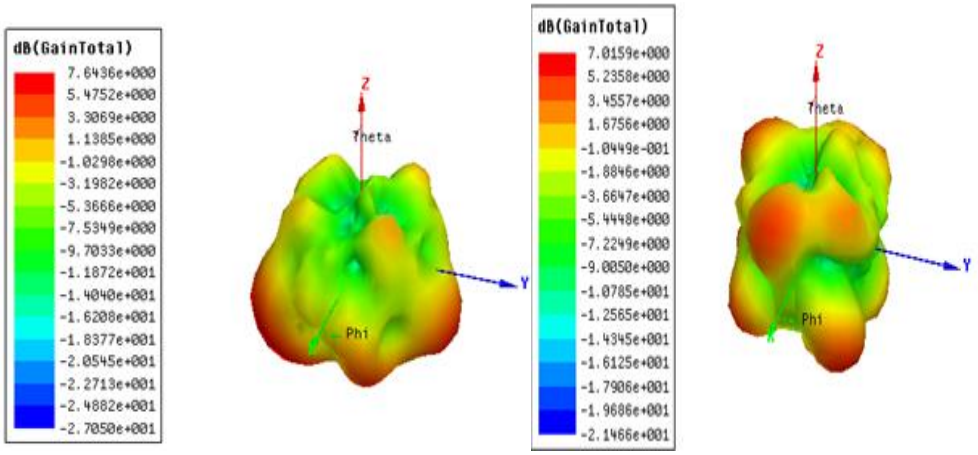
dB(GainTotal)
7.6436e+000
5.4752e+000
3.3069e+000
1.1385e+000
-1.0298e+000
-3.1982e+000
-5.3666e+000
-7.5349e+000
-9.7033e+000
-1.1872e+001
-1.4040e+001
-1.6208e+001
-1.8377e+001
-2.0545e+001
-2.2713e+001
-2.4882e+001
-2.7050e+001
Z
Theta
Y
Phi
dB(GainTotal)
7.0159e+000
5.2358e+000
3.4557e+000
1.6756e+000
-1.0449e-001
-1.8846e+000
-3.6647e+000
-5.4448e+000
-7.2249e+000
-9.0050e+000
-1.0785e+001
-1.2565e+001
-1.4345e+001
-1.6125e+001
-1.7906e+001
-1.9686e+001
-2.1466e+001
Z
Theta
Y
Phi

(c) (d)

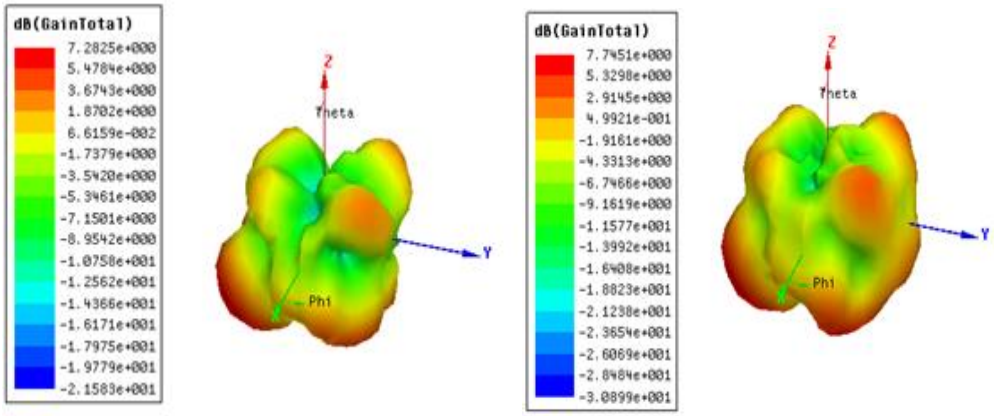
dB(GainTotal)
7.2825e+000
5.4784e+000
3.6743e+000
1.8702e+000
6.6159e-002
-1.7379e+000
-3.5420e+000
-5.3461e+000
-7.1501e+000
-8.9542e+000
-1.0758e+001
-1.2562e+001
-1.4366e+001
-1.6171e+001
-1.7975e+001
-1.9779e+001
-2.1583e+001
Z
Theta
Y
Phi
dB(GainTotal)
7.7451e+000
5.3298e+000
2.9145e+000
4.9921e-001
-1.9161e+000
-4.3313e+000
-6.7466e+000
-9.1619e+000
-1.1577e+001
-1.3992e+001
-1.6408e+001
-1.8823e+001
-2.1238e+001
-2.3654e+001
-2.6069e+001
-2.8484e+001
-3.0899e+001
Z
Theta
Y
Phi

(e) (f)

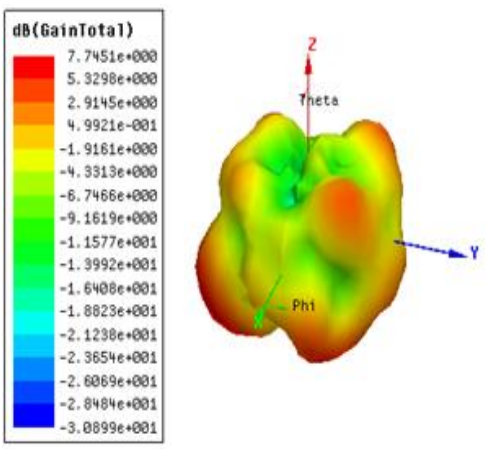
dB(GainTotal)
7.7451e+000
5.3298e+000
2.9145e+000
4.9921e-001
-1.9161e+000
-4.3313e+000
-6.7466e+000
-9.1619e+000
-1.1577e+001
-1.3992e+001
-1.6408e+001
-1.8823e+001
-2.1238e+001
-2.3654e+001
-2.6069e+001
-2.8484e+001
-3.0899e+001
Z
Theta
Y
Phi

(g)

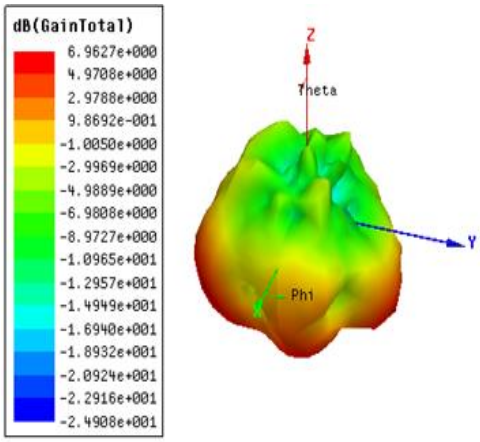
dB(GainTotal)
6.9627e+000
4.9708e+000
2.9788e+000
9.8692e-001
-1.0050e+000
-2.9969e+000
-4.9889e+000
-6.9808e+000
-8.9727e+000
-1.0965e+001
-1.2957e+001
-1.4949e+001
-1.6940e+001
-1.8932e+001
-2.0924e+001
-2.2916e+001
-2.4908e+001
Z
Theta
Y
Phi

(h)

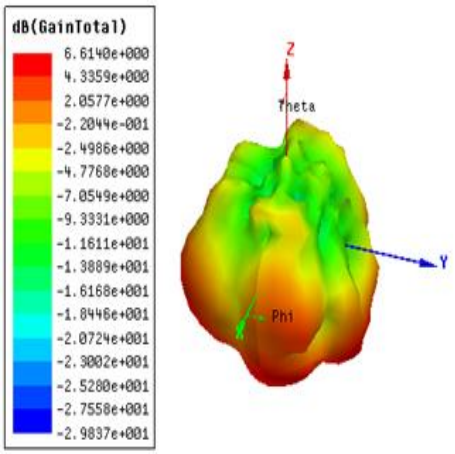
dB(GainTotal)
6.6140e+000
4.3359e+000
2.0577e+000
-2.2044e-001
-2.4986e+000
-4.7768e+000
-7.0549e+000
-9.3331e+000
-1.1611e+001
-1.3889e+001
-1.6168e+001
-1.8446e+001
-2.0724e+001
-2.3002e+001
-2.5280e+001
-2.7558e+001
-2.9837e+001
Z
Theta
Y
Phi

(i)

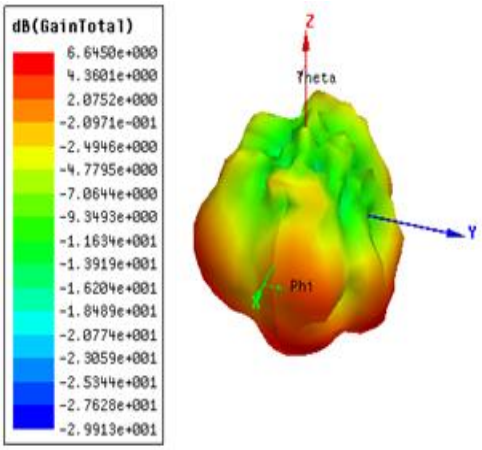
dB(GainTotal)
6.6450e+000
4.3601e+000
2.0752e+000
-2.0971e-001
-2.4946e+000
-4.7795e+000
-7.0644e+000
-9.3493e+000
-1.1634e+001
-1.3919e+001
-1.6204e+001
-1.8489e+001
-2.0774e+001
-2.3059e+001
-2.5344e+001
-2.7628e+001
-2.9913e+001
Z
Theta
Y
Phi

(j)

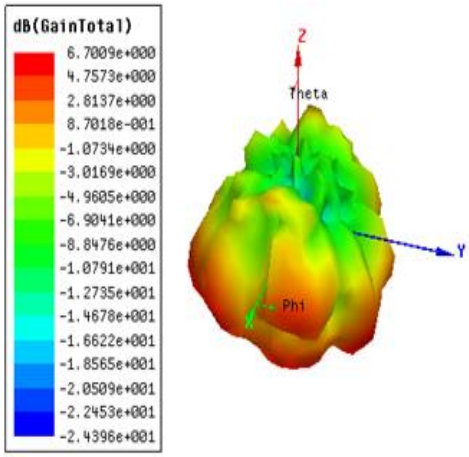
dB(GainTotal)
6.7009e+000
4.7573e+000
2.8137e+000
8.7018e-001
-1.0734e+000
-3.0169e+000
-4.9605e+000
-6.9041e+000
-8.8476e+000
-1.0791e+001
-1.2735e+001
-1.4678e+001
-1.6622e+001
-1.8565e+001
-2.0509e+001
-2.2453e+001
-2.4396e+001
Z
Theta
Y
Phi

(k)

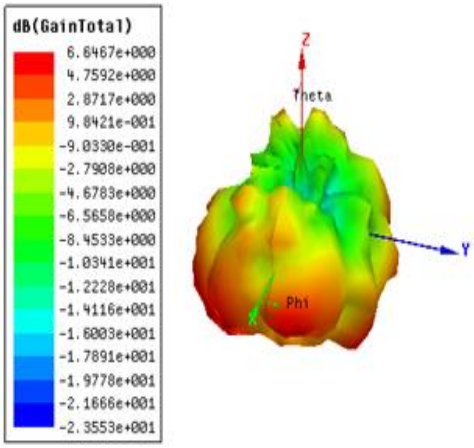
dB(GainTotal)
6.6467e+000
4.7592e+000
2.8717e+000
9.8421e-001
-9.0330e-001
-2.7908e+000
-4.6783e+000
-6.5658e+000
-8.4533e+000
-1.0341e+001
-1.2228e+001
-1.4116e+001
-1.6003e+001
-1.7891e+001
-1.9778e+001
-2.1666e+001
-2.3553e+001
Z
Theta
Y
Phi

(l)

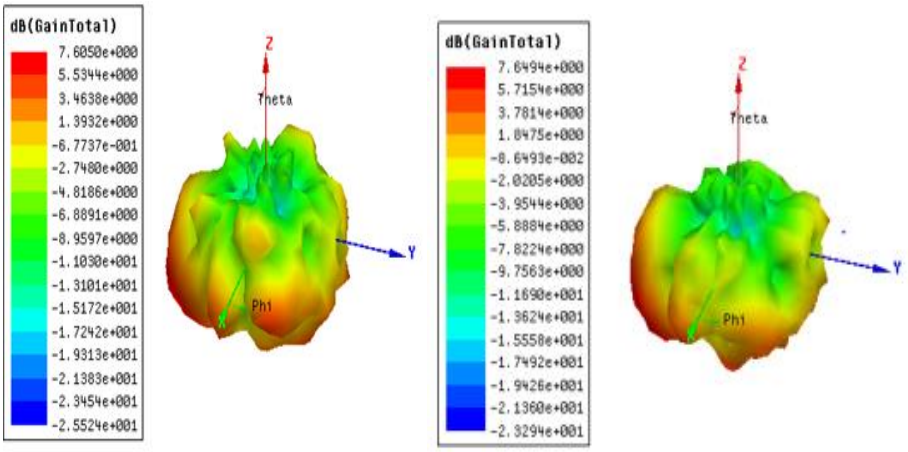

(m) (n)

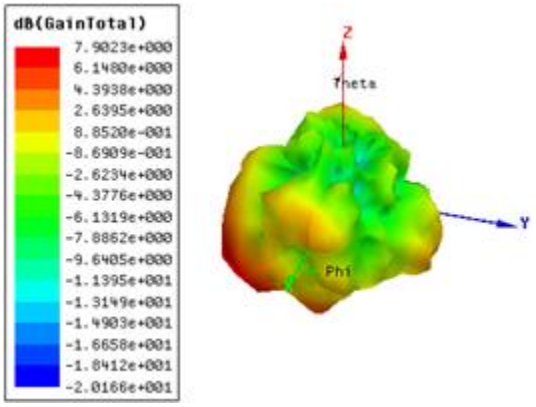

(o)

Figure 3.13 3D Gain plot of antenna with FSS at (a) 16.75 GHz (b) 14.5 GHz and (c) 19 GHz (d) 12 GHz (e) 12.5(f) 13GHz (g) 13.5 GHz (h) 14 GHz (i) 15 GHz (j) 15.5 GHz (k) 16 GHz (l) 16.5 GHz (m) 17.5 GHz (n) 18 GHz (o) 20 GHz

radiating source. Aperture coupled micro-strip patch antenna acts as a radiating source is designed in one step and in the second step the FSS superstrate layer is designed and then the radiating source is analyzed under the effect of FSS superstrate layer. The proposed micro-strip patch antenna is shown in Fig. 3.10.

The s-parameters of the antenna is shown in shown in figure 3.11. The result shows that it's covering the frequency band from 12 Ghz to 20 GHz.

The 3D peak gain plots of antenna with FSS has been presented in figure 3.13. The result shows that the overall gain of the antenna has been increased after the addition of FSS structure.

The bistatic RCS of antenna with FSS is shown in figure 3.15. The main lobe magnitude is -64.9 dBm at operating frequency 16 GHz for theta 90° is shown in figure 3.14(a). The main lobe magnitude at 20 GHz is -65 dBm, whereas side lobe level is -0.7 dB as shown in figure 3.14(b).

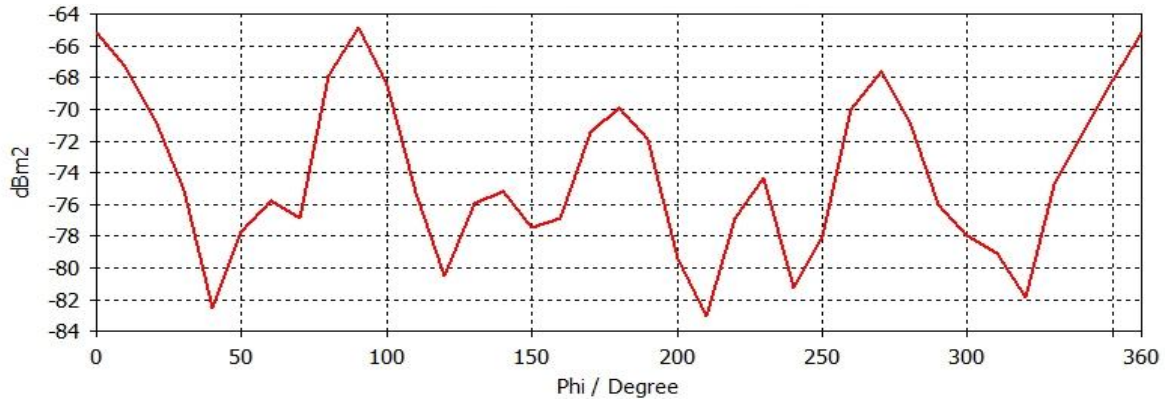

(a)

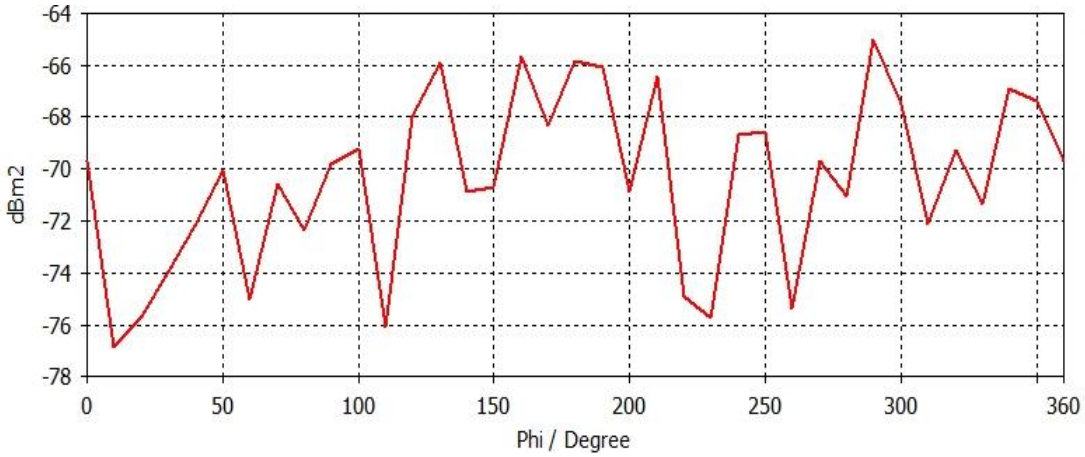

(b)

Figure 3.14 RCS plot for theta 90°(a) 16 GHz and (b) 20 GHz

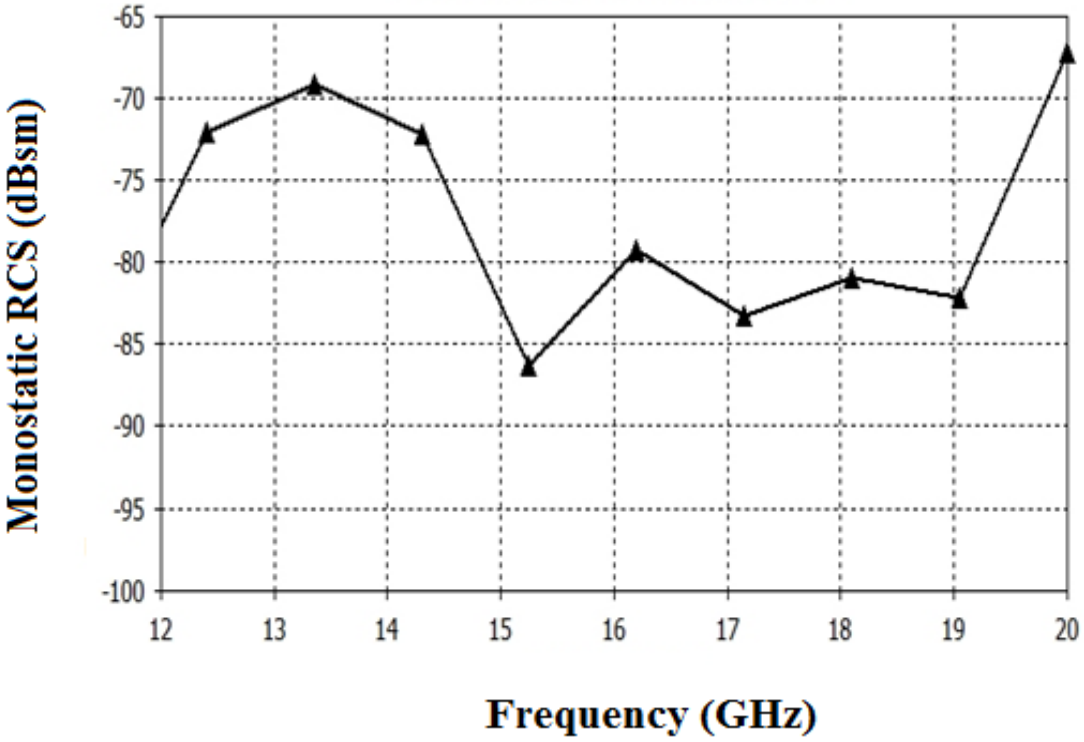

Figure 3.15 Monostaic radar cross section of antenna with FSS

The figure 3.15 shows that the RCS is reduced over the frequency range from 15.2 GHz to 19.1 GHz, the value of RCS at 15.2 GHz is -86 dB , at 17.15 GHz it is -80.25 dB, at 19.1 GHz the value of RCS is -81 dB.

CHAPTER 4

Design Analysis of Antenna with FSS

The designed antenna and frequency selective surface (FSS) is fabricated as discussed in the previous chapter. Simulated results has been compared with the measured results and good agreement has been observed. Peak gain of antenna with and without FSS has been discussed and radar cross section (RCS) in dBsm has been presented. The proposed antenna with FSS has been compared with the existed literature at the end of the chapter.

4.1 Antenna Design

After the design of the antenna in HFSS software the next stage was to fabricate and measure the results of simulated antenna. In order to keep the size constraints of the micro-strip patch antenna and to achieve the reduced radar cross section (RCS), the final design comprises of 8×8 array FSS. Since the main goal of the project was to design a micro-strip patch antenna with reduced radar cross section, this was the suitable substitution.

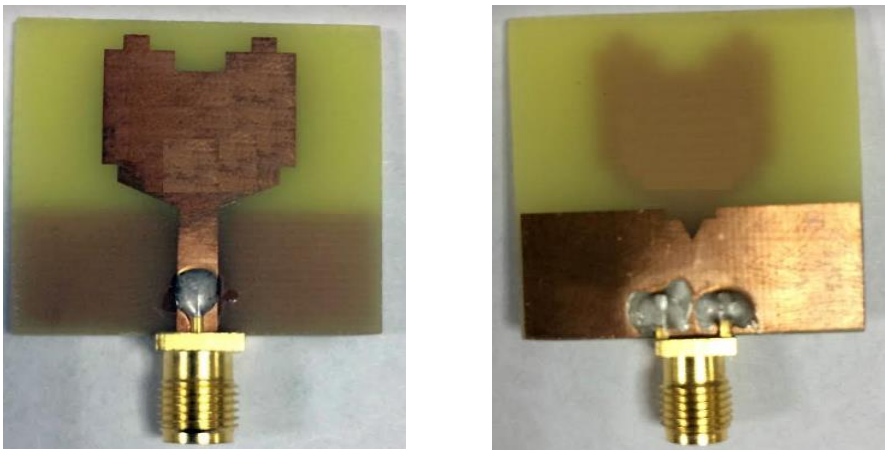

(a) (b)

Figure 4.1 Fabricated UWB Antenna (a) Front View (b) Back View

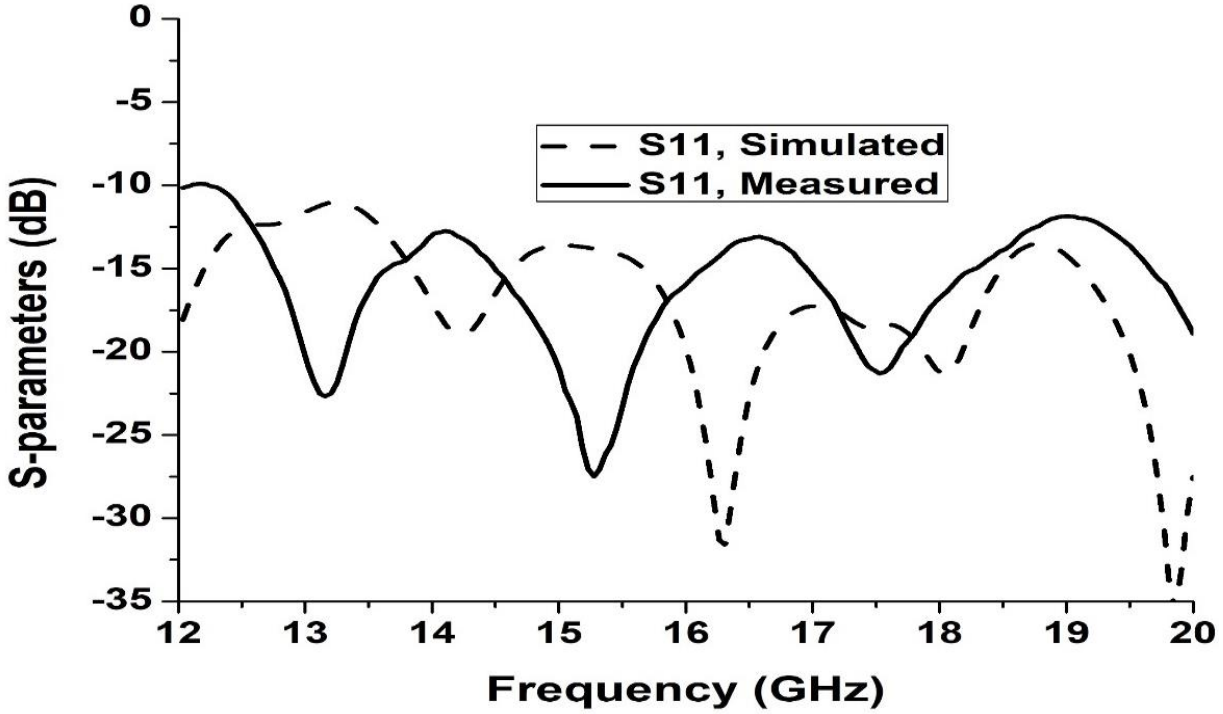

Figure 4.2 UWB Antenna simulated and measured results

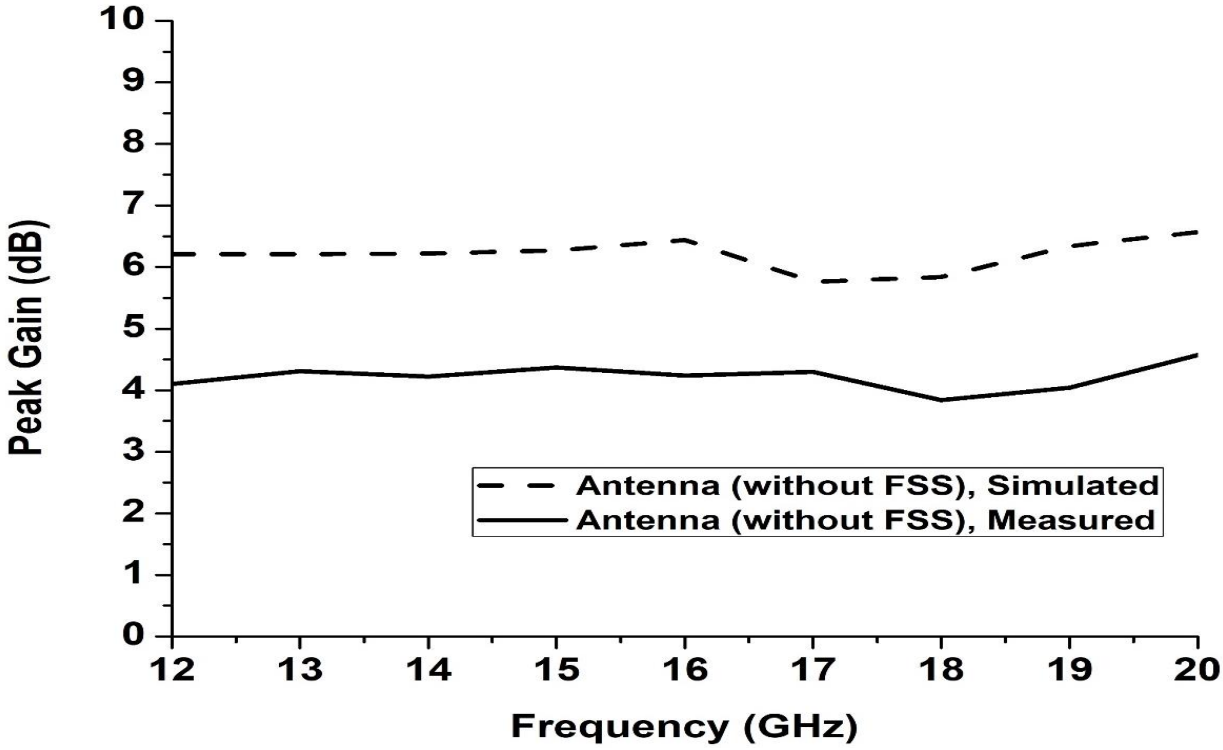

Figure 4.3 Peak gain of UWB Antenna without FSS

The proposed prototype was fabricated on FR4 dielectric substrate with 1 mm thickness, loss tangent of 0.02, for supporting the FSS layer foam is placed between the radiating patch and FSS layer. The resemblance of the simulated and measured result shows that the insulation foam has a very minor affect. The fabricated hardware of the micro-strip patch antenna is shown in Fig. 4.1.

4.2 FSS Design

After designing the unit cell FSS array are studied, the total dimensions of FSS array are 62.5 × 62.5 mm^2. The array factor under the normal incidence of the plan wave can be classified as [42]:

$$AF = \sum_{y=1}^{Y}\sum_{z=1}^{Z} exp\left\{j\left\{(y-1/2)(kd\sin\theta\cos\Phi) + \left(z-\frac{1}{2}\right)(kd\sin\theta\sin\Phi) + \varphi(y,z)\right\}\right\}$$

In this equation θ is the elevation angel and φ is the azimuth angle, while d and φ y, z represents

Figure 4.4 Fabricated 8 × 8 frequency selective surface (FSS)

the distance between the elements and the initial phase of the lattice, respectively. FSS array of 8×8 is chosen because it is providing the better gain than 4×4 array.

4.3 Antenna with FSS

FSS is placed above the antenna at a seperation distance of 4 mm to achieve high peak gain at the

Figure 4.5 Antenna with FSS at a seperation distance of 4 mm

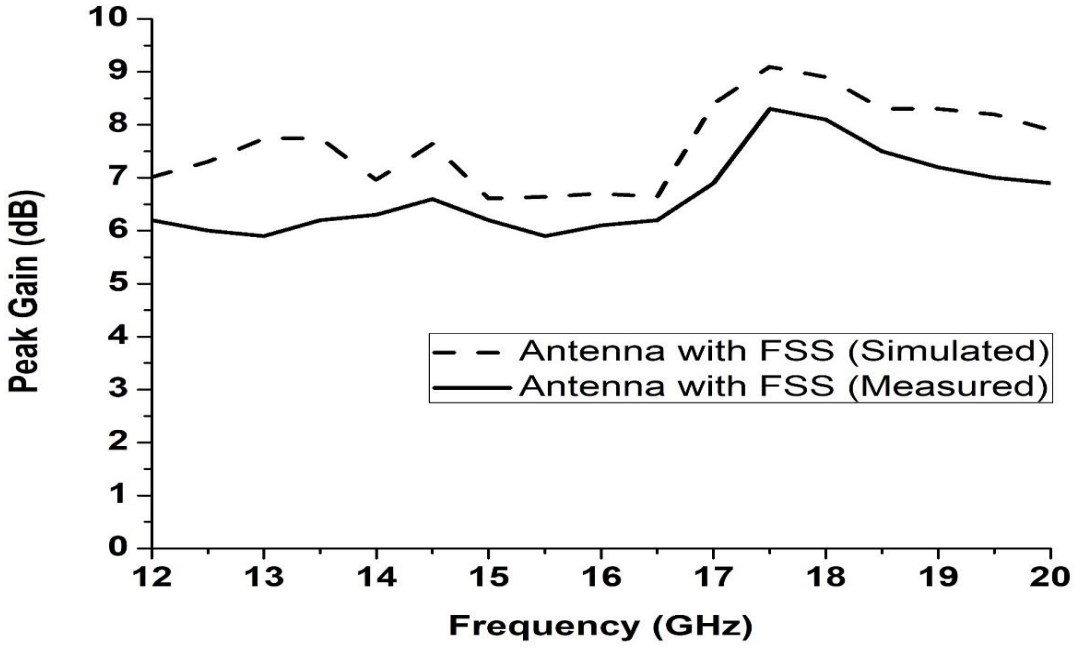

Figure 4.6 Peak gain of antenna with FSS

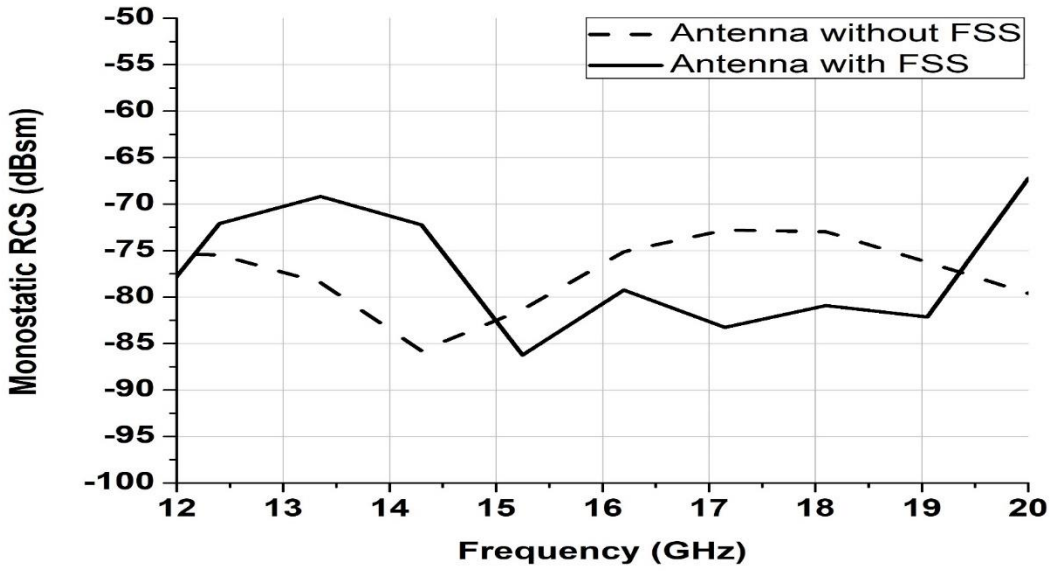

Figure 4.7 Monostaic radar cross section of antenna with FSS and without FSS

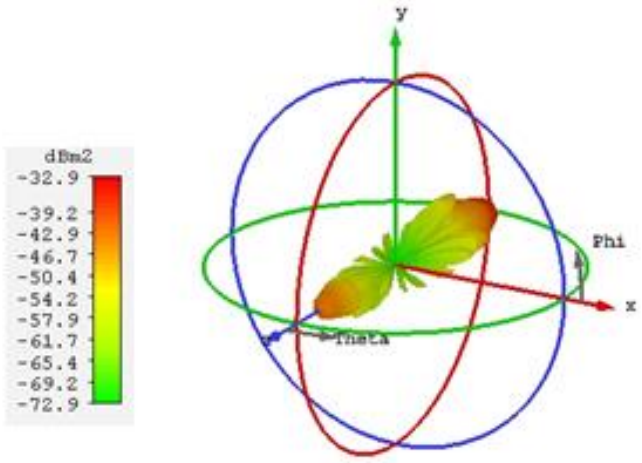

Figure 4.8 3D RCS of antenna with FSS at 16 GHz

operation frequency bands as shown in figure 4.5. Simulated results has been compared with the measure results as illustrated in figure 4.6. Measured results showed that the peak gain 8.1 dB has been observed at 17.5 GHz. The average gain of antenna with FSS is 6.1 dB. Monostatic

radar cross section (RCS) has been presented in figure 4.7. The result shows that maximum RCS -87.5 dBsm has been observed at 15.2 GHz. Minimum RCS -67.6 dBsm has been observed at 20 GHz. Three dimensional (3D) RCS of antenna with FSS has been presented in figure 4.8.

The proposed antenna with FSS has been compared with the existed literature as shown in table 4.1. It has been observed that our proposed structure is compact than [22], [24] and [25]. Whereas the impedance bandwidth of our proposed antenna is better than [23].

REF NO.	ANTENNA WORKING FREQUENCY	DIMENSIONS	RCS REDUCED FREQUENCY RANGE	IN-BAND OR OUT OF BAND RCS REDUCTION	PEAK RCS REDUCTION OBTAINED
[22]	7 GHz	70×60 mm^2	2.5-18 GHz	In-band	4.7 GHz
[23]	12 GHz	50×50 mm^2	8-24 GHz	In-band & out of band	18 GHz
[24]	3.47 GHz	85.8×85.8 mm^2	2-20 GHz	In-band	20 GHz
[25]	8 GHz	70×60 mm^2	3.6-16 GHz	In-band	14 GHz
PROP.	5.7 GHz	62.5×62.5 mm^2	12-20 GHz	In-band	15.2 GHz

Table 4.1 Comparison of proposed work with the existed literature

Chapter 5

CONCLUSION AND FUTURE WORK

5.1 Discussion

Highly effective and reliable antennas are required by stealth applications and for the easy installation these antennas are need to be compact in size and should have low profile. For the achievement of reduced radar cross section (RCS) ,high gain, compactness, reduced circuitry and low losses, FSS are used as a superstrate over the antenna for the enhancement of gain and directivity. The patch antenna is designed for the stealth applications. For this at the first step the novel FSS layer is designed for which FSS unit cell and then the array of these cells is designed. After designing the FSS it is then placed above the antenna and is studied, analyzed and fabricated. A good agreement between the simulated and fabricated results is shown in this work.

5.2 Conclusion

The antenna with FSS that is proposed in this thesis covers the frequency band from 12 to 20 GHz.. Firstly the simple patch antenna was designed then the changes are done in the ground plan to achieve the good results. Then the unit cell is designed for the FSS and master-slave boundaries are assigned to it. The unit cell is duplicated along both the axis to make a 8×8 FSS. The whole sheet of FSS is placed above the antenna. The proposed antenna design will be prove useful in stealth applications, in detecting devices and it is also useful for the military platforms while minimizing the overall budget.

5.3 Future work

- No doubt the results achieved in this thesis are excellent, but for every research there always exists a room for advancement, so following directions can be focused for further research in the proposed area of interest.
- The RCS reduction is achieved from 15 GHz to 19 GHz from the proposed antenna. The work can be done towards the RCS reduction for the entire Ku/K band.
- For wide frequency band operation, and for compact size, many other feeding techniques like inset feeding, coaxial probe and coupled feed can be introduced.

BIBLIOGRAPHY

[1] H. Nikookar and R. Prasad, "Introduction to ultra wideband for wireless communications," vol. 200: *Springer*, 2009.

[2] H. G. Schantz, "A brief history of UWB antennas," *IEEE Aerospace and Electronic Systems Magazine*, vol. 19, pp. 22-26, 2004.

[3] Federal Communication Commission, Washington, DC, USA, "Revision of part 15 of the Commissions rule regarding ultra-wideband transmission systems FCC 0248," *First Report and Order*, Feb. 2002.

[4] M. N. Shakib, M. Moghavvemi, W. N.L. Mahadi, "A Low-Profile Patch Antenna for Ultrawideband Application," *IEEE Antennas And Wireless Propagation Letters*, vol 14,2015.

[5] Y. Zhou, X. Cao, J. Gao, S. Li, Y. Zheng, "In-Band RCS Reduction and Gain Enhancement of a Dual-Band PRMS-Antenna," *IEEE Antennas And Wireless Propagation Letters*, vol. 16, pp.2716-2720,2017.

[6] H. Jiang, Z. Xue, M. Leng, W. Li, W. Ren, "Wideband partially reflecting surface antenna with broadband RCS reduction," *IET Microwave Antennas propagation.*, vol 12, pp. 941-946, 2017.

[7] Z.J. Han, W. Song, X. Q. Sheng, "Gain Enhancement and RCS Reduction for Patch Antenna by using Polarization-Dependent EBG Surface," *IEEE Antennas And Wireless Propagation Letters*, vol. 16, pp. 1631-1634, 2017.

[8] Y. Liu, H. Wang, Y. Jia, S. Gong, "Broadband Radar Cross-Section Reduction for Microstrip

Patch Antenna Based on Hybrid AMC Structures," *Progress In Electromagnetics Research*, vol. 50, pp. 21-28,2014.

[9] Y. Han, J. Wang, S. Gong, Y. Li,Y. Zhang, J. Zhang, "Low RCS Antennas Based on Dispersion Engineering of Spoof Surface Plasmon Polaritons," *IEEE Transactions On Antennas And Propagation*, vol. 66, pp. 7111-7116,2018.

[10] J. Mu, H. Wang, H. Wang, Y. Huang, "Low-RCS and Gain Enhancement Design of a Novel Partially Reflecting and Absorbing Surface Antenna," *IEEE Antennas And Wireless Propagation Letters*, vol. 16, pp. 1903-1906, 2017.

[11] H. B. Baskey, E. Johari, M. J. Akhtar, "Metamaterial Structure Integrated With a Dielectric Absorber for Wideband Reduction of Antennas Radar Cross Section," *IEEE Transaction On Electromagnetic Compatibility*, vol. 59, pp. 1060-1069,2017.

[12] P. Mei, X. Q. Lin, J. W. Yu, A. Boukarkar, P. C. Zhang, Z. Q. Yang, "Development of a Low Radar Cross Section Antenna With Band-Notched Absorber," *IEEE Transactions On Antennas And Propagation*, vol. 66,pp.582-589,2018.

[13] Islam, M. Tariqul, R. Azim,A. T. Mobashsher,"Triple band-notched planar UWB antenna using parasitic strips," *Progress In Electromagnetics Research* 129, pp. 161-179, 2012.

[14] K. P. Ray, "Design Aspects of Printed Monopole Antennas for Ultra-Wide Band Applications," *International Journal of Antennas and Propagation*, pp. 1-8, 2008.

[15] Santos, R. A., and S. Cerqueira Jr., "A low-profile and ultra-wideband printed antenna with a 176% bandwidth," *Journal of Microwaves, Optoelectronics and Electromagnetic Applications*, vol. 16,pp. 59-69, 2017.

[16] Rakhi and S. Thakur, "Performance Analysis of Different Shapes Patch Antennas at 2.45 GHz," *International Journal of Engineering Research and Technology*, vol.3, Issue 9, 2014.

[17] K.Anusudha, and M. Karmugil,"Design of circular microstip patch antenna for ultra wide band applications," Proceedings of IEEE International Conference on *Control, Instrumentation, Communication and Computational Technologies (ICCICCT),* pp. 304-308, 2016.

[18] Deshmukh, Amit A., et al., "Ultra-wideband modified rectangular microstrip antenna," *Proceedings of Online International Conference on Green Engineering and Technologies (IC-GET),* pp. 1-4, 2016.

[19] J. Liu, S. Zhong and K. P. Esselle, "A printed elliptical monopole antenna with modified feeding structure for bandwidth enhancement," *IEEE Transactions on Antennas and Propagation*, vol. 59, Issue 2, pp. 667-670, 2011.

[20] M. P. Abegaonkar, et al.,"Tapered-CPW fed printed triangular monopole antenna," Antennas and Propagation EuCAP, 2006.

[21] T. Mandal, and S. Das,"A coplanar waveguide fed hexagonal shape ultra wide band antenna with WiMAX and WLAN band rejection," *Radioengineering Journal*, vol.23, Issue 4, pp. 1077-1085, 2014.

[22] C. M. Dikmen, S. Cimen, and G. Cakir, "Planar octagonal-shaped UWB antenna with reduced radar cross section," *IEEE Trans. Antennas Propagation*, vol. 62, Issue 6, pp. 2946-2953, 2014.

[23] S. Singhal, T. Goel, and A. K. Singh, "Novel diamond shaped UWB monopole antenna,"

Annual IEEE India Conference (INDICON) ,2013.

[24] L. Lizzi, R. Azaro ; G. Oliveri ; A. Massa,"Printed UWB antenna operating over multiple mobile wireless standards," *IEEE Antennas and Wireless Propagation Letters*, vol. 10,pp. 1429-1432, 2011.

[25] T.K. Wu, "Frequency Selective Surface and Grid Array," New York, Wiley, 1995.

[26] R. Mittra, C.H. Chan and T. Cwik, "Techniques for Analyzing Frequency Selective Surfaces A Review," *Proceedings of the IEEE*, vol. 76, Issue 12, pp. 1593-1615, 1988.

[27] F. Bayatpur, "Metamaterial-Inspired Frequency-Selective Surfaces", *Thesis University of Michigan*, 2009.

[28] G. Marconi and C.S. Franklin, "Reflector for use in wireless telegraphy and telephony," U.S. Patent, 1,301,473 1919.

[29] B.A. Munk, "Frequency-selective surfaces: Theory and design," Wiley, New York, 2000.

[30] D. Pozar, "Microwave Engineering," pp. 125-160, third edition, Wiley, New York, 2004.

[31] C. M. Dikmen , S. Çimen , G. Çakır, "Planar Octagonal-Shaped UWB Antenna With Reduced Radar Cross Section," *IEEE Transactions on Antennas and Propagation*, vol. 62, Issue 6, 2014.

[32] Y. Liu , Y. Hao ,H. Wang , K. Li , S. Gong, "Low RCS Micro-strip Patch Antenna Using Frequency-Selective Surface and Micro-strip Resonator," *IEEE Antennas and Wireless Propaga*tion letters, vol. 14, pp. 1290 - 1293, 2015.

[33] Y. W. Hao, Y. Liu, K. Li, and S. Gong, "Wideband radar crosssection reduction of microstrip

patch antenna with split-ring resonators," Electron. Letter, vol. 51, Issue 20, pp. 1608–1609, 2015.

[34] S. S. Parit, V. G. Kasabegoudar, "Ultra Wideband Antenna with Reduced Radar Cross Section," *International Journal of Electromagnetics and Applications*, vol. 6, Issue 2, pp. 23-30, 2016.

[35] Y. Liu, Y. Hao, K. Li, S. Gong, "Radar Cross Section Reduction of a Micro-strip Antenna Based on Polarization Conversion Meta-material," *IEEE Antennas and Wireless Propagation Letters*, vol. 15, 2016.

[36] Z. J. Han, W. Song, X, Q. Sheng, "Gain Enhancement and RCS Reduction for Patch Antenna by Using Polarization-Dependent EBG Surface," *IEEE Antennas and Wireless Propagation Letters*, vol. 16, 2017.

[37] A. Shater and D. Zarifi, "Radar cross section reduction of microstrip antenna using dual-band metamaterial absorber," *ACES Journal*, vol. 32, Issue 2, pp. 135-140, 2017.

[38] Y. Zhou, X. Cao, J. Gao, S. Li, and Y. Zheng, "In-band RCS reduction and gain enhancement of a dual-band PRMS-antenna," *IEEE Antennas Wireless Propagation Letter* , vol. 16, pp. 2716–2720, 2017.

[39] M. Pazokian, N. Komjani, M. Karimipour, "Broadband RCS Reduction of Microstrip Antenna Using Coding Frequency Selective Surface," *IEEE Antennas and Wireless Propagation Letters*, vol. 17, Issue 8, pp. 1382-1385, 2018.

[40] Abbas pirhadi, Hadi Bahrami and Javad nasir "Wideband high directive aperture coupled microstrip antenna design by using a FSS superstrate layer*," IEEE Trans. Antennas Propagation*, vol. 60, no.4, April 2012.

[41] M. Mateen Hassan , Maryam Rasool , M. Umair Asghar, Zeeshan Zahid , Adnan Ahmed Khan, Imran Rashid, Abdul Rauf and Farooq Ahmed Bhatti, "A novel UWB MIMO antenna array with band notch characteristics using parasitic de-coupler,"*Journal of Electro magnatic Waves and Applications*,23,October 2019.

[42] J. Li, T. Ali Khan, X. Meng, J. Chen, G. Peng, A. Zhang, "Wideband Radar Cross Section Reduction of Microstrip patch antenna using Coding Metasurface," *IET Microwaves, Antenna Propagation*,17 April 2019.